cells were isolated from mice. Cynomolgus ES cells and their differentiated progenitors were used as targets. Spleen cells were mixed with target cells at a ratio of 5:1 to 40:1 and incubated for 4 h at 37°C. The supernatant was examined for the release of lactate dehydrogenase using a Cytotoxicity Detection Kit (Takara, Shiga, Japan). Percent cytotoxicity was calculated as follows: cytotoxicity (%) = (experimental value − low control) × 100/(high control − low control). Low and high controls were obtained after incubating target cells alone or with 1% Triton X-100, respectively. The percent cytotoxicity was indicated as average values from assays performed in triplicate.

RESULTS

There is considerable variation among reports regarding the number of ES cells needed for teratomas to form in mice: from 10–15 clumps (200 cells) per site (18) to 5×10^6 cells per site (30). First, we examined how many nonhuman primate ES cells are necessary to generate teratomas in mice. In all transplantation experiments, we used cynomolgus ES cells expressing GFP (CMK6G) to detect the transplanted cells and track their fate in vivo. As recipient mice, we used two immunodeficient strains: NOD/SCID and NOG mice. NOG mice are more immunodeficient than NOD/SCID mice: NK as well as T and B cells are absent in NOG mice, although NK cells are present in NOD/SCID mice. Cynomolgus ES cells usually grow as clusters. When the cells were transplanted as clumps (not dissociated into single cells) into the limb muscle of NOG and NOD/SCID mice, teratomas developed in all mice that were transplanted with 1×10^5 or more cells, but they were observed only in some of the mice that were transplanted with 1×10^4 and 5×10^3 cells. Teratomas were not observed in any mice transplanted with 1×10^3 cells (Table 1). A similar cell–dose dependency was observed regardless of the mouse strains.

To see whether cellular state affects the tumorigenesis, cynomolgus ES cells as clumps or dissociated cells were transplanted into the lower limb muscle in NOD/SCID mice. As previously reported for human ES cells (18,24), cynomolgus ES cells also exhibit poor plating efficiency. During subculturing, limited dissociation with 0.1% collagenase (to maintain clumps of 10–50 cells) is recommended to enable continued growth (21). As expected, the number of ES cells necessary for teratomas to form in all mice was different: 5×10^4 for clumps and 5×10^5 for single cells (Table 1, Fig. 1). A larger number of ES cells was required for single cells than clumps to form a teratoma.

ES cells have been transplanted into different sites: subcutaneously into the hind leg muscle, testis capsule, abdominal cavity, etc., for teratoma-forming assays. To detremine whether the site affects tumorigenesis, ES cells (as clumps) were transplanted into the lower limb muscle or subcutaneously into the back in NOD/SCID mice. The number of ES cells necessary for teratomas to develop in all mice differed: 5×10^4 for the lower limb muscle and 5×10^5 for the subcutis in the back (Table 1, Fig. 1).

Teratoma-forming assays are often performed to test the safety of ES cell-derived progenitor preparations. To prepare cynomolgus ES cell-derived hematopoietic precursor cells, ES cells were cultured for 6 days to induce the hematopoietic differentiation. On day 6, the expression of CD34, VEGFR2, and Scl was upregulated, but CD45 was not yet expressed (data not shown). Therefore, day 6 cells likely included hematopoietic precursor cells (20,26,28). After the 6-day culture, 85% of cells were still positive for SSAE-4, an undifferentiated marker of both human and nonhuman primate ES cells (24,25) (data not shown). These cells (1×10^6) were transplanted into the lower limb muscle in NOG and NOD/SCID mice. Notably, the incidence of tumorigenesis differed between the two strains. Teratomas devel-

Table 1. Formation of Teratomas in Immunodeficient Mice

	Recipient Mouse Strain			
Transplanted Cell No.	NOD/SCID (Clumps/Muscle)*	NOG (Clumps/Muscle)	NOD/SCID (Dissociated Cells/Muscle)	NOD/SCID (Clumps/Subcutis)
1×10^6	**3/3**	**3/3**	**3/3**	**3/3**
5×10^5	**3/3**		**3/3**	**3/3**
1×10^5	**3/3**	**3/3**	2/3	2/3
5×10^4	**3/3**		1/3	2/3
1×10^4	1/3	2/3	0/3	0/3
5×10^3	0/3		0/3	0/3
1×10^3	0/3	0/3	0/3	0/3

Bold type indicates the formation of teratomas in all mice.
*Indicates cellular state/transplant site.

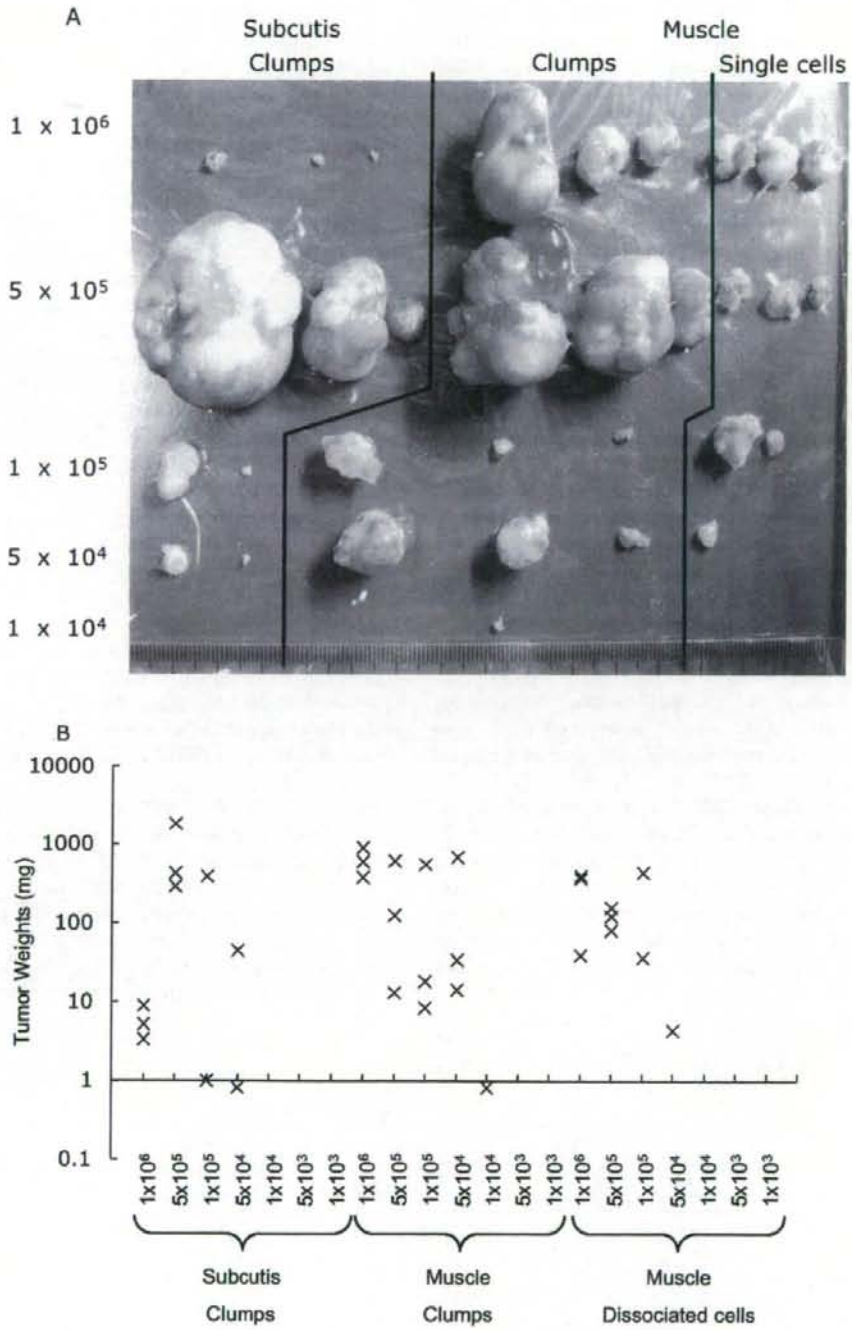

Figure 1. Formation of teratomas dependent on cell number and state. Cynomolgus ES cells (1×10^3 to 1×10^6 per site) were transplanted into NOD/SCID mice. The cells, either as clumps or dissociated single cells, were injected subcutaneously into the back or intramuscularly into the lower limb. Dissected tumors (A) and their weights (B) are shown.

Table 2. Formation of Teratomas Dependent on Recipients

Transplanted Cells	NOD/SCID	NOG	Fetal Sheep*	Fetal Monkeys†	Immunosuppressed Adult Monkeys‡
Cynomolgus ES cells (undifferentiated)	5/5	3/3	4/15	3/3	NT
Cynomolgus ES cell-derived progenitors	2/5	5/5	1/10	3/3	2/2

NT, not tested.
*As published in Tanaka et al. (23).
†As published in Shibata et al. (20).
‡As published in Nara et al. (15). In this experiment, cynomolgus ES cell-derived neural precursor cells were transplanted. In other experiments, cynomolgus ES cell-derived hematopoietic precursor cells were transplanted.

oped in all NOG mice (5/5). However, they developed in only two of five NOD/SCID mice (Table 2), despite that 85% of the transplanted cells (8.5×10^5) were positive for SSEA-4, which should have been enough for teratomas to form in terms of the number of undifferentiated ES cells transplanted (Table 1).

The innate immunity of the recipient mice was then evaluated. It turned out that the cytotoxic activity of spleen cells (putative NK cell activity) in the mice was greater against the ES cell-derived progenitors than undifferentiated ES cells (Fig. 2), suggesting that ES cell-derived progenitor cells are more immunogenic than undifferentiated ES cells.

Histological examination revealed that, in NOD/SCID mice, neutrophils (as Gr-1 positive) were already present around the grafts on day 1 after transplantation, but they had disappeared and were replaced by dendritic cells/active NK cells (as CD45/B220 positive) and macrophages (as BM8 positive) by day 3 (Fig. 3). These immune cells likely eliminated the transplanted cells, presumably more vigorously when ES cell-derived progenitor cells were transplanted (as suggested from Fig. 2), resulting in the failure of teratomas to develop in some NOD/SCID mice as shown in Figure 3 (detected only in two out of five NOD/SCID mice as shown in Table 2).

A similar failure to detect tumorigenesis was also noted in fetal sheep (23) (Table 2). On the other hand, teratomas developed in all monkeys, whether fetal monkeys or immunosuppressed adult monkeys, tested in the

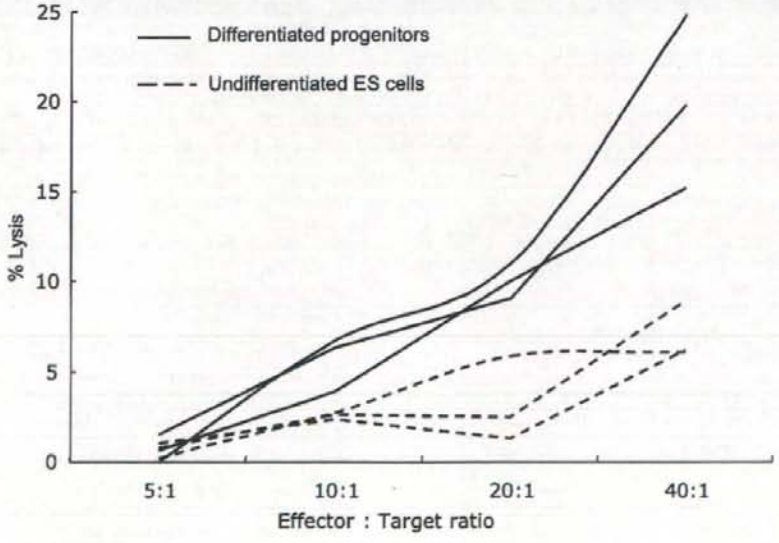

Figure 2. Cytotoxic activity against ES cells and their differentiated progenitors. Effectors: spleen cells of NOD/SCID mice. Targets: cynomolgus ES cells or their differentiated progenitors (hematopoietic precursor cells). The cytotoxic activity of mouse spleen cells (putative NK cell activity) was found to be stronger against the ES cell-derived progenitors than undifferentiated ES cells.

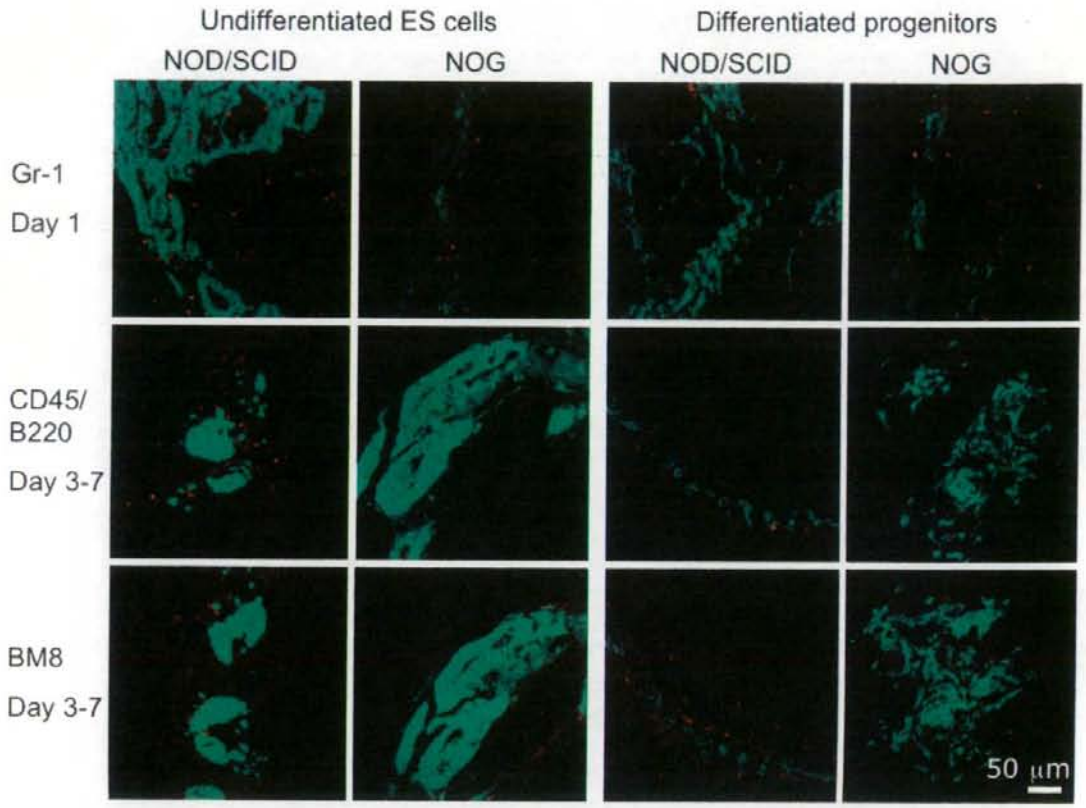

Figure 3. Immune responses to transplanted cells. Cynomolgus ES cells or their differentiated progenitors (1×10^6 cells) were transplanted into the hind leg muscle in NOD/SCID and NOG mice. Gr-1-positive cells (as neutrophils) were present on day 1 (upper panel) but disappeared by day 3. Instead, CD45/B220-positive cells (as plasmacytoid dendritic cells and active NK cells) and BM8-positive cells (as macrophages) were present around the transplanted cells and progeny after day 3, especially in NOD/SCID mice, resulting in the failure of engraftment (middle and lower panels). Green shows GFP-positive transplanted cells and their progeny. Gr-1, CD45/B220, and BM8 were stained in red.

allogeneic settings (15,20) (Table 2), even though the inclusion of the GFP gene in transplanted cells might enhance the immune response.

DISCUSSION

This study showed that the incidence with which teratomas form after cynomolgus ES cells are transplanted into immunodeficient mice is highly variable and depends on several conditions. First, the number of cells transplanted is critical. A similar result was reported for the allogeneic transplantation of mouse ES cells (16). Transplanted ES cells may be liable to apoptosis due to physical stress and environmental changes at transplantation, or they may be eliminated by innate immunity including neutrophils and macrophages present even in immunodeficient mice, as shown in Figure 3. Taking into account the apoptosis and clearance of cells post-transplant, a sufficient number of ES cells (1×10^5 or more) must be transplanted to assess the ability to form teratomas.

Second, teratomas developed much less frequently after the transplantation of dissociated ES cells than of cell clumps; that is, a larger number of ES cells is required for single cells than clumps to form a teratoma. This may be related to the finding that human ES cells are liable to apoptosis upon cellular dissociation (1,17, 18,24). They undergo massive cell death, particularly after complete dissociation, and the cloning efficiency of dissociated human ES cells is generally very low (<1%) (8,29,31). Therefore, cellular state is also important when transplanting ES cells to form teratomas.

Third, the transplant site also affected the formation

of teratomas. One-log larger numbers of ES cells were needed for teratomas to develop after subcutaneous compared to intramuscular transplantation. Connective tissue is sparse in the subcutis compared to muscle, and thus cells transplanted into the subcutis may disperse and so an adequate regional density cannot be retained. Similarly, it has been reported that larger numbers of pancreatic β-cells (9) and tumor cells (11,12) survived after intramuscular than subcutaneous transplantations. In addition, no teratoma was noted at all after intraperitoneal injection, even of 1×10^6 ES cells (data not shown), which should be enough to generate teratomas in the muscle (Table 1). Alternatively, in the muscle, blood flow is abundant and high concentrations of various factors are available for the survival and proliferation of transplanted cells, and thus the muscle may provide conditions more favorable for the tumorigenesis.

Another point is that the host immunity is related to the tumorigenesis. In fact, phagocytes were present around ES cells soon after transplantation in both NOG and NOD/SCID mice. Notably, teratomas developed more frequently in NOG mice (Table 2), in which NK as well as T and B cells were absent, than in NOD/SCID mice, in which NK cells were present. The presence of NK cells in NOD/SCID mice might be attributable to the lower incidence of teratomas. Thus, host innate immunity should be considered when assessing the formation of teratomas.

Finally, regarding the tumorigenesis of ES cell-derived progenitors, the incidence of teratomas posttransplant was very different depending on the recipient mice. We have shown that when ES cell-derived hematopoietic precursor cells (of which 85% were still positive for SSEA-4) were transplanted into NOD/SCID mice, teratomas only developed in some of the animals tested. However, teratomas developed in all NOG mice after the transplantation of these same cells. Furthermore, teratomas developed in all NOG mice even with ES cell-derived progenitor cells of which only 2% were positive for SSEA-4 (data not shown). Therefore, when ES cell-derived progenitors are subjected to an assay of tumorigenesis in vivo using NOD/SCID mice (instead of NOG mice), the risk of tumors developing will likely be underestimated. A predictive assay to detect the tumorigenesis of progenitor cell preparations prior to clinical application is critically important. In this regard, unlike other xenogeneic recipients, either NOD/SCID mice or fetal sheep, NOG mouse recipients closely reflect the results of tumorigenesis in the allogeneic monkey recipients (Table 2), and thus NOG mice should be useful as recipients to predict the tumorigenesis of ES cell-derived progenitor preparations.

We have previously shown that the risk of tumor formation was considerably high after transplantation of monkey ES cell-derived progenitor cells in the allogeneic setting (15,20). In fact, teratomas developed in all monkeys, whether fetal monkeys or immunosuppressed adult monkeys, tested in the allogeneic settings (Table 2). It has been considered that residual pluripotent cells are responsible for the tumor formation posttransplant (4,20). If that is the case, why didn't the residual pleuripotent cells in the ES cell-derived progenitor preparations form teratomas in every NOD/SCID mouse (Table 2)? We and others have shown that immunogenicity increases with the differentiation of ES cells (7) (Fig. 2). The differentiated cell population expressed potent immunogens, which might have functioned as adjuvants. As a result, the residual undifferentiated fraction might be eventually rejected together with the differentiated fraction.

In conclusion, the present study demonstrated that several factors (cell number, cellular state, transplant site, differentiation state, and mouse strain) would affect whether teratomas form after the transplantation of nonhuman primate ES cells and their progenitors into immunodeficient mice. These factors must be taken into consideration when examining the pluripotency of ES cells and, more importantly, when addressing the safety of ES cell-derived progenitor preparations.

ACKNOWLEDGMENTS: We are grateful to Naohide Ageyama (Tsukuba Primate Research Center, Ibaraki, Japan) for his technical help. We thank Norio Nakatsuji (Kyoto University, Kyoto, Japan) and Yasushi Kondo (Mitsubishi Tanabe Pharma Corporation, Osaka, Japan) for providing cynomolgus ES cells. We also thank Toru Nakano (Osaka University, Osaka, Japan) for providing OP9. This study was supported by grants (JMS 21st Century COE Program, High-tech Research Center Program, and KAKENHI) from the Ministry of Education, Culture, Sports, Science and Technology of Japan as well as grants (KAKENHI) from the Ministry of Health, Labor and Welfare of Japan. Y. Kishi is a JSPS Research Fellow. There is no financial conflict regarding the authors.

REFERENCES

1. Amit, M.; Carpenter, M. K.; Inokuma, M. S.; Chiu, C. P.; Harris, C. P.; Waknitz, M. A.; Itskovitz-Eldor, J.; Thomson, J. A. Clonally derived human embryonic stem cell lines maintain pluripotency and proliferative potential for prolonged periods of culture. Dev. Biol. 227:271–278; 2000.
2. Asano, T.; Ageyama, N.; Takeuchi, K.; Momoeda, M.; Kitano, Y.; Sasaki, K.; Ueda, Y.; Suzuki, Y.; Kondo, Y.; Torii, R.; Hasegawa, M.; Ookawara, S.; Harii, K.; Terao, K.; Ozawa, K.; Hanazono, Y. Engraftment and tumor formation after allogeneic in utero transplantation of primate embryonic stem cells. Transplantation 76:1061–1067; 2003.
3. Ballas, Z. K.; Rasmussen, W. Lymphokine-activated killer cells. VII. IL-4 induces an NK1.1+CD8 alpha+beta– TCR-alpha beta B220+ lymphokine-activated killer subset. J. Immunol. 150:17–30; 1993.
4. Bieberich, E.; Silva, J.; Wang, G.; Krishnamurthy, K.; Condie, B. G. Selective apoptosis of pluripotent mouse

and human stem cells by novel ceramide analogues prevents teratoma formation and enriches for neural precursors in ES cell-derived neural transplants. J. Cell Biol. 167:723–734; 2004.
5. Bjorck, P. Isolation and characterization of plasmacytoid dendritic cells from Flt3 ligand and granulocyte-macrophage colony-stimulating factor-treated mice. Blood 98: 3520–3526; 2001.
6. Chen, Y.; Soto-Gutierrez, A.; Navarro-Alvarez, N.; Rivas-Carrillo, J. D.; Yamatsuji, T.; Shirakawa, Y.; Tanaka, N.; Basma, H.; Fox, I. J.; Kobayashi, N. Instant hepatic differentiation of human embryonic stem cells using activin A and a deleted variant of HGF. Cell Transplant. 15:865–871; 2006.
7. Drukker, M.; Katz, G.; Urbach, A.; Schuldiner, M.; Markel, G.; Itskovitz-Eldor, J.; Reubinoff, B.; Mandelboim, O.; Benvenisty, N. Characterization of the expression of MHC proteins in human embryonic stem cells. Proc. Natl. Acad. Sci. USA 99:9864–9869; 2002.
8. Hasegawa, K.; Fujioka, T.; Nakamura, Y.; Nakatsuji, N.; Suemori, H. A method for the selection of human embryonic stem cell sublines with high replating efficiency after single-cell dissociation. Stem Cells 24:2649–2660; 2006.
9. Juang, J. H.; Hsu, B. R.; Kuo, C. H. Islet transplantation at subcutaneous and intramuscular sites. Transplant. Proc. 37:3479–3481; 2005.
10. Kim, D. S.; Kim, J. Y.; Kang, M.; Cho, M. S.; Kim, D. W. Derivation of functional dopamine neurons from embryonic stem cells. Cell Transplant. 16:117–123; 2007.
11. Klaunig, J. E.; Barut, B. A. Influence of transplantation site on metastatic ability of mouse bladder carcinoma sublines. J. Urol. 140:844–847; 1988.
12. Klaunig, J. E.; Barut, B. A. Role of the implantation site on metastatic ability of the murine MBT-2 transitional cell carcinoma. Urol. Res. 16:19–21; 1988.
13. Nakano, T.; Kodama, H.; Honjo, T. Generation of lymphohematopoietic cells from embryonic stem cells in culture. Science 265:1098–1101; 1994.
14. Nakayama, T.; Momoki-Soga, T.; Yamaguchi, K.; Inoue, N. Efficient production of neural stem cells and neurons from embryonic stem cells. Neuroreport 15:487–491; 2004.
15. Nara, Y.; Muramatsu, S.; Takino, N.; Kodera, M.; Nakayama, T.; Inoue, N.; Kakiuchi, T.; Tukada, H.; Ono, H.; Terao, K.; Okuno, T.; Konishi, N.; Konishi, N.; Suzuki, Y.; Kondo, Y.; Nito, S. Brain tumor formation after allogeneic transplantation of monkey embryonic stem cells. Neuropathology 25(2):17; 2005.
16. Nussbaum, J.; Minami, E.; Laflamme, M. A.; Virag, J. A.; Ware, C. B.; Masino, A.; Muskheli, V.; Pabon, L.; Reinecke, H.; Murry, C. E. Transplantation of undifferentiated murine embryonic stem cells in the heart: teratoma formation and immune response. FASEB J. 21:1345–1357; 2007.
17. Pyle, A. D.; Lock, L. F.; Donovan, P. J. Neurotrophins mediate human embryonic stem cell survival. Nat. Biotechnol. 24:344–350; 2006.
18. Reubinoff, B. E.; Pera, M. F.; Fong, C. Y.; Trounson, A.; Bongso, A. Embryonic stem cell lines from human blastocysts: Somatic differentiation in vitro. Nat. Biotechnol. 18: 399–404; 2000.
19. Sasaki, K.; Nagao, Y.; Kitano, Y.; Hasegawa, H.; Shibata, H.; Takatoku, M.; Hayashi, S.; Ozawa, K.; Hanazono, Y. Hematopoietic microchimerism in sheep after in utero transplantation of cultured cynomolgus embryonic stem cells. Transplantation 79:32–37; 2005.
20. Shibata, H.; Ageyama, N.; Tanaka, Y.; Kishi, Y.; Sasaki, K.; Nakamura, S.; Muramatsu, S.; Hayashi, S.; Kitano, Y.; Terao, K.; Hanazono, Y. Improved safety of hematopoietic transplantation with monkey embryonic stem cells in the allogeneic setting. Stem Cells 24:1450–1457; 2006.
21. Suemori, H.; Tada, T.; Torii, R.; Hosoi, Y.; Kobayashi, K.; Imahie, H.; Kondo, Y.; Iritani, A.; Nakatsuji, N. Establishment of embryonic stem cell lines from cynomolgus monkey blastocysts produced by IVF or ICSI. Dev. Dyn. 222:273–279; 2001.
22. Takada, T.; Suzuki, Y.; Kondo, Y.; Kadota, N.; Kobayashi, K.; Nito, S.; Kimura, H.; Torii, R. Monkey embryonic stem cell lines expressing green fluorescent protein. Cell Transplant. 11:631–635; 2002.
23. Tanaka, Y.; Nakamura, S.; Shibata, H.; Kishi, Y.; Ikeda, T.; Masuda, S.; Sasaki, K.; Abe, T.; Hayashi, S.; Kitano, Y.; Nagao, Y.; Hanazono, Y. Sustained macroscopic engraftment of cynomolgus embryonic stem cells in xenogeneic large animals after in utero transplantation. Stem Cells Dev. 17:367–382; 2008.
24. Thomson, J. A.; Itskovitz-Eldor, J.; Shapiro, S. S.; Waknitz, M. A.; Swiergiel, J. J.; Marshall, V. S.; Jones, J. M. Embryonic stem cell lines derived from human blastocysts. Science 282:1145–1147; 1998.
25. Thomson, J. A.; Kalishman, J.; Golos, T. G.; Durning, M.; Harris, C. P.; Becker, R. A.; Hearn, J. P. Isolation of a primate embryonic stem cell line. Proc. Natl. Acad. Sci. USA 92:7844–7848; 1995.
26. Umeda, K.; Heike, T.; Yoshimoto, M.; Shiota, M.; Suemori, H.; Luo, H. Y.; Chui, D. H.; Torii, R.; Shibuya, M.; Nakatsuji, N.; Nakahata, T. Development of primitive and definitive hematopoiesis from nonhuman primate embryonic stem cells in vitro. Development 131:1869–1879; 2004.
27. Wang, J.; Murakami, T.; Yoshida, S.; Matsuoka, H.; Ishii, A.; Tanaka, T.; Tobita, K.; Ohtsuki, M.; Nakagawa, H.; Kusama, M.; Kobayashi, E. Predominant cell-mediated immunity in the oral mucosa: Gene gun-based vaccination against infectious diseases. J. Dermatol. Sci. 31:203–210; 2003.
28. Wang, L.; Li, L.; Shojaei, F.; Levac, K.; Cerdan, C.; Menendez, P.; Martin, T.; Rouleau, A.; Bhatia, M. Endothelial and hematopoietic cell fate of human embryonic stem cells originates from primitive endothelium with hemangioblastic properties. Immunity 21:31–41; 2004.
29. Watanabe, K.; Ueno, M.; Kamiya, D.; Nishiyama, A.; Matsumura, M.; Wataya, T.; Takahashi, J. B.; Nishikawa, S.; Nishikawa, S.; Muguruma, K.; Sasai, Y. A ROCK inhibitor permits survival of dissociated human embryonic stem cells. Nat. Biotechnol. 25:681–686; 2007.
30. Xu, C.; Inokuma, M. S.; Denham, J.; Golds, K.; Kundu, P.; Gold, J. D.; Carpenter, M. K. Feeder-free growth of undifferentiated human embryonic stem cells. Nat. Biotechnol. 19:971–974; 2001.
31. Zwaka, T. P.; Thomson, J. A. Homologous recombination in human embryonic stem cells. Nat. Biotechnol. 21:319–321; 2003.

Int. J. Dev. Biol. [in Press]
(Use DOI or consult the journal web for the definitive reference of this article)

THE INTERNATIONAL JOURNAL OF DEVELOPMENTAL BIOLOGY
www.intjdevbiol.com

Large-scale production of growing oocytes *in vitro* from neonatal mouse ovaries

ARATA HONDA[1,#], MICHIKO HIROSE[1,#], KIMIKO INOUE[1,4], HITOSHI HIURA[2,##], HIROMI MIKI[1], NARUMI OGONUKI[1], MICHIHIKO SUGIMOTO[1], KUNIYA ABE[1], MITO KANATSU-SHINOHARA[3], TOMOHIRO KONO[2], TAKASHI SHINOHARA[3] and ATSUO OGURA[*,1,4,5]

[1]*Bioresource Center, RIKEN, Tsukuba, Ibaraki,* [2]*Department of BioScience, Tokyo University of Agriculture, Setagaya-ku, Tokyo,* [3]*Department of Molecular Genetics, Graduate School of Medicine, Kyoto University, Kyoto,* [4]*Graduate School of Life and Environmental Sciences, University of Tsukuba, Tsukuba, Ibaraki and* [5]*The Center for Disease Biology and Integrative Medicine, Faculty of Medicine, University of Tokyo, Bunkyo-ku, Tokyo, Japan*

ABSTRACT Although fetal or neonatal mammalian ovaries contain many non-growing oocytes within primordial follicles, most degenerate and only a few contribute to the oocyte pool in the mature ovary. Here, we report a follicle-free culture system that allows a large number of these arrested oocytes to enter the growth phase *in vitro*. As many as 800 oocytes from a newborn mouse, corresponding to more than 10^4 oocytes in large animals, continued to develop, formed a zona pellucida, and were able to fuse with spermatozoa. Some oocytes reached the size of those in normal antral follicles and entered metaphase I, indicating the completion of the growth phase. The key to success was the sequential provision of essential nutrients and growth factors to the oocytes, while preventing the apoptosis that normally occurs in the majority of growing oocytes *in vivo*. Importantly, maternal genomic imprinting, which is necessary for normal embryonic development, was imposed correctly on their genomes autonomously. Thus, arrested primordial oocytes can be rescued effectively *in vitro* and can undergo the morphological and genomic modifications necessary for fertilization and subsequent embryonic development. This culture system may provide a significant impetus to the development of new techniques for the efficient production of oocytes from fetal or neonatal ovaries, for research, clinical, and zoological purposes.

KEY WORDS: *theca cell, follicle, stem cell factor, genomic imprinting*

Introduction

Mammalian oogenesis starts in the female fetus. When primordial germ cells or oogonia reach the fetal gonads and become oocytes, they become arrested at the diplotene stage of meiotic prophase I. They are packaged into primordial follicles, consisting of a single layer of granulosa cells, during the late fetal stages in many domestic species, or just after birth in mice, and remain in these small follicles until they enter the growth phase (Hirshfield, 1991; van den Hurk and Zhao, 2005). When the primordial oocytes start to grow and proceed through the different stages of development, they undergo a progressive series of morphological and genomic modifications. It is clear that during their development—especially in the growth phase—follicle cell support is essential to provide the oocytes with nutrients and metabolic regulators. This is why the follicular structure is critical for the induction of oocyte growth *in vitro*. Indeed, oocytes grow poorly or degenerate during culture when they are separated from granu-

Abbreviations used in this paper: ESM, embryonic stem cell medium; GSM, germline stem cell medium; SCF, stem cell factor.

***Address correspondence to:** Atsuo Ogura. Bioresource Center, RIKEN, 3-1-1, Tsukuba, Ibaraki 305-0074, Japan. Fax: +81-29-836-9172. e-mail: ogura@rtc.riken.go.jp

Supplementary Material for this paper (two figures) is available at: http://dx.doi.org/10.1387/ijdb.082607ah

Notes: #These authors contributed equally. ##Current address: Departments of Obstetrics and Gynecology, Tohoku University Graduate School of Medicine, Sendai, Japan.

Accepted: 12 May 2008. *Published online:* 12 January 2009.

ISSN: Online 1696-3547, Print 0214-6282
© 2009 UBC Press
Printed in Spain

losa cells (Brower and Schultz, 1982; Haghighat and Van Winkle, 1990). *In vitro* oocyte growth systems are most advanced in mouse models, with the successful production of normal offspring from the primordial oocytes of newborn mice (Eppig and O'Brien, 1996) or from fetal germ cells using nuclear exchange techniques (Obata and Kono, 2002). Thus, primary oocytes can complete their growth phase to resume meiosis and undergo fertilization if the follicular cells nurse the oocytes correctly.

Despite these advances, the numbers of growing oocytes obtained during *in vitro* growth experiments are significantly lower than the numbers of primary oocytes found in neonatal ovaries (more than 2,000 at two days after birth; Canning *et al.*, 2003). This is primarily attributable to the programmed cell death (apoptosis) of the oocytes during culture, which also occurs normally during follicular atresia in developing ovaries (De Felici *et al.*, 2005). Mechanical and enzymatic damage to the oocytes at the time of ovary dissection and the inadequacy of culture conditions might also reduce the number of living oocytes. Thus, the efficient production of growing oocytes *in vitro* depends on the development of better methods of isolating primordial oocytes from ovaries and the optimization of conditions for the growth of oocytes *in vitro*. However, the complexity of the developmental orchestration of the oocytes and the surrounding follicular cells has been an obstacle to the precise analysis of the events controlling oogenesis. An ideal oocyte culture system would be one in which the oocytes undergo normal growth without any supporting cells in a defined culture milieu, so that the direct effects of factors on oocyte development can be determined precisely.

Recently, we found that crude suspensions of neonatal ovarian cells form round spherical colonies under serum-free conditions when the adherent cells are depleted from the culture. The colonies are composed exclusively of putative thecal stem cells and primordial oocytes (Honda *et al.*, 2007). With the addition of a stem cell factor (SCF, c-Kit ligand) to the medium, naked oocytes are released from the colonies individually or as germ cell cysts. This study was undertaken to test whether these freed oocytes can develop *in vitro* without supporting cells and whether they can be used for the sorts of biochemical analyses that are usually difficult to perform in the presence of somatic cell contaminants. The somatic-cell-free culture system developed in this study and the information obtained from it may lead to a better understanding of the mechanisms underlying oogenesis and provide some clues to the development of new systems for efficient oocyte production *in vitro*.

Results

Preparation and culture of oocytes

We have previously reported a method of isolating putative thecal stem cells from newborn mouse ovaries through selective culture (Honda *et al.*, 2007). With this method, granulosa cells and other adherent cells (mostly fibroblast cells) were depleted from the culture, which was confirmed by the lack of expression of their marker genes (Honda *et al.*, 2007). The remaining thecal stem cells formed free spherical colonies when they were cultured in serum-free germline stem cell medium (GSM). Many of the primordial oocytes that had existed in the ovaries were incorporated into these colonies. As the thecal stem cells proliferated and the colonies increased in size, the oocytes inside the colonies started to protrude from the surface after 8–10 days in culture. The presence of SCF did not affect the timing of oocyte protrusion, but it apparently increased their numbers on the surfaces of the colonies (data not shown). The oocytes became detached from the colonies individually or as germ cell cysts (Pepling and Spradling, 2001; Fig. 1A, B). The oocytes released into the medium were about 15–20 μm in diameter and had no granulosa cells or zona pellucida (ZP). They were all inferred to be preexisting oocytes because they had previously stained positively for the germ cell marker, mouse vasa homologue (MVH), and produced a negative result in a cell proliferation assay (Honda *et al.*, 2007). The oocytes started to grow without any supporting somatic cells in the same culture medium containing SCF (Fig. 1C). They reached about 35 μm in diameter and formed a ZP within 16–20 days (Fig. 1D). They retained normal chromosomal integrity, as indicated by the formation of tetrad chromosomes after the induction of chromosomal condensation within the MII ooplasm (Supplementary Figure 1). The 5-bromo-2'-deoxyuridine (BrdU)-incorporation assay demonstrated that the protruding oocytes

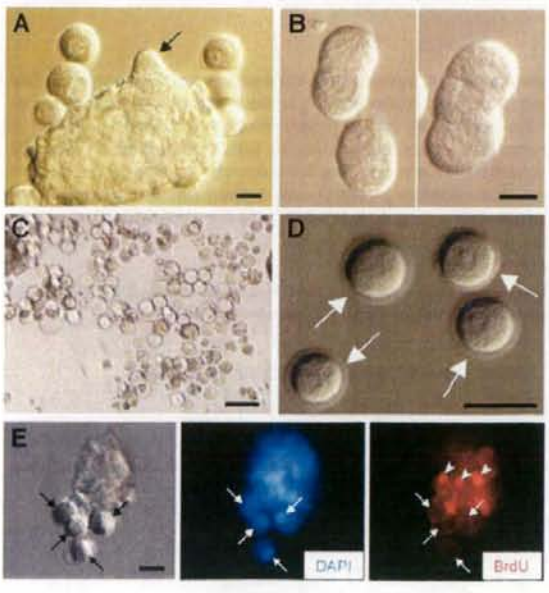

Fig. 1. Mouse oocytes emerging from thecal stem cell colonies. *Primordial oocytes protruded from the surfaces of thecal stem cell colonies (arrows in A) and were released individually* **(A)** *or as germline cysts* **(B)**. *The germline cysts on the right consist of four oocytes, each of which is slightly larger than those on the left. The released oocytes continued to develop without follicular cell support* **(C)** *and formed the ZP (arrows in* **(D)**). *Oocytes emerging from colonies were most likely preexisting prophase I oocytes because they showed no signs of proliferation (BrdU-negative; arrows in* **(E)**). *The thecal stem cells in the colony were BrdU-positive, indicating their active proliferation and DNA synthesis (arrowheads in E). The oocytes were deformed during the fixation and staining processes. Scale bars: 20 μm (A, B, D, and E) and 100 μm (D). Hoffman interference contrast optics images.*

were completely negative, whereas the cells in the colonies were stained, reflecting the incorporation of BrdU into their DNA (Fig. 1E). Thus, these SCF-responsive oocytes were derived from preexisting mitotically inactive oocytes, and not from any presumptive female germline stem cells (Johnson *et al.*, 2004).

In another series of experiments, we prepared ovarian cell suspensions from 4-, 9-, and 14-day-old female mice and cultured them in parallel. Thecal cell colonies and naked oocytes were collected from each group, but their numbers apparently decreased with the age of the mice. Even under optimized culture conditions (see below), about 200 and 50 oocytes were collected from each female in the 9- and 14-day-old groups, respectively, whereas more than 800 were recovered from the four-day-old group.

Optimization of oocyte culture conditions

As mentioned above, SCF treatment accelerated both the derivation of the oocytes from thecal cell colonies and their subsequent growth *in vitro*. We then examined whether different SCF concentrations altered the oocyte growth kinetics. The final size of the oocytes depended on the concentration of SCF. Throughout the observation period (28 days), the greatest effect of SCF on oocyte diameter was observed at the highest concentrations (50 and 100 ng/ml; Fig. 2A). The numbers of oocytes released from the colonies also increased in parallel with the SCF concentration (Fig. 2B) during the first 20 days, with about four times more oocytes at 50 ng/ml and 100 ng/ml SCF than in the controls (no SCF) or with 5 ng/ml SCF. However, many of the oocytes cultured at 100 ng/ml SCF started to degenerate at day 20 and most had been lost by day 28 (Fig. 2B). Thus, as far as we investigated, the best results in terms of the numbers and sizes of the living oocytes were obtained when they were cultured in 50 ng/ml SCF. Most oocytes that underwent degeneration in culture were terminal deoxynucleotidyl transferase (TdT)-mediated dUTP nick-end-labeling (TUNEL) positive (Fig. 2C), irrespective of their size and the day of culture, indicating that apoptosis occurred in these oocytes as it does during atresia *in vivo*.

We confirmed that the oocytes growing *in vitro* without somatic cells expressed Kit as well as other oocyte-specific genes, including Zp1 (zona pellucida 1) and Mvh (mouse vasa homolog; Fig. 3A), similar to oocytes growing *in vivo*. Kit receptors were also

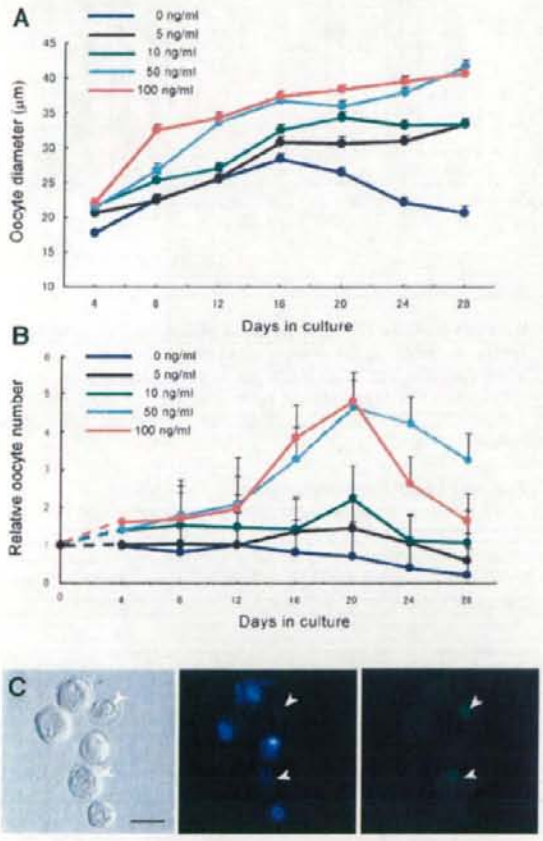

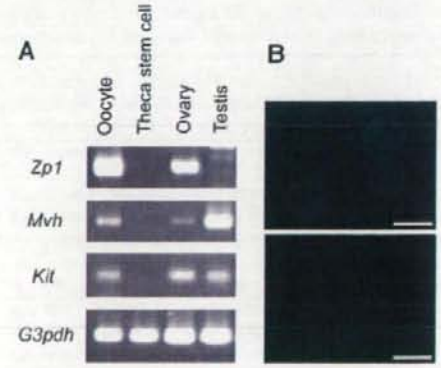

Fig. 2 (Left). Effects of stem cell factor (SCF) on the development of oocytes *in vitro*. **(A)** *The mean oocyte diameter increased with days in culture, reaching a maximum size at 50 or 100 ng/ml of SCF.* **(B)** *The numbers of oocytes (> 30 μm in diameter) released from the colonies increased until day 20 of culture, but thereafter they decreased with oocyte death. Throughout culture, 50 ng/ml SCF gave the best results in terms of the sizes and survival rates of the oocytes.* **(C)** *Oocytes underwent degeneration by apoptotic cell death, as detected by TUNEL staining. Apoptotic oocytes (arrowheads) were labeled with FITC (green on the right) but not with Hoechst dye (blue in the middle). The oocytes were deformed during the fixation and staining processes. Scale bar: 20 μm.*

Fig. 3 (Right). Gene expression patterns of growing oocytes and the localization of the Kit receptors on the oocyte surface. **(A)** *Oocytes growing in vitro without somatic cells correctly expressed three oocyte marker genes, Zp1, Mvh, and Kit. The testicular tissue also expressed Mvh and Kit. Thecal cells did not express Kit because they were in the stem cell state and very immature.* **(B)** *Kit receptor proteins were clearly localized on the surfaces of oocytes growing in vitro by staining with a specific antibody (upper). Oocytes stained with normal goat serum showed no fluorescence (bottom).*

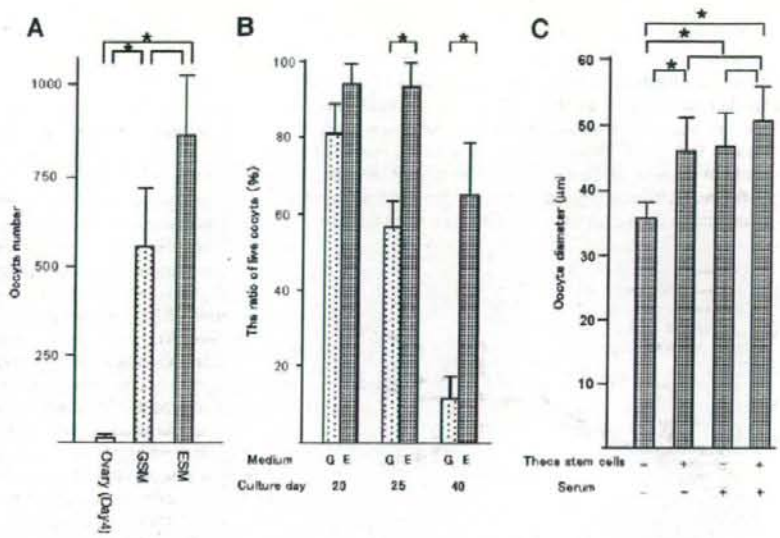

Fig. 4. Effects of basal medium, thecal stem cells, and serum on the development of oocytes. (A) *The mean numbers of oocytes obtained from the ovaries of neonates reached more than 800 after 22 days of culture when embryonic stem cell medium (ESM) was used as the basal medium (significantly different from the germline stem cell medium (GSM) group; P < 0.001).* **(B)** *ESM also sustained the survival of the oocytes better than did GSM. The survival rates were significantly different between the two groups at 25 and 40 days (P < 0.001).* **(C)** *Effects of thecal stem cells and serum on oocyte diameter. Thecal stem cells and serum synergistically accelerated the development of the oocytes. Error bars represent the SD. The lines connecting two bars indicate statistically significant differences between values at P < 0.01 (without asterisk) or P < 0.001 (with asterisk).*

correctly localized on the surfaces of these growing oocytes (Fig. 3B).

We initially used GSM as the basal medium for the *in vitro* growth of oocytes because this medium had been used successfully for the isolation and culture of thecal stem cells (Honda *et al.*, 2007). However, we found that a simpler medium, embryonic stem cell medium (ESM) with SCF but without serum, gave better results. Significantly, better grown oocytes (> 30 μm diameter) were obtained with ESM than with GSM (861.0 ± 62.9 vs. 553.6 ± 59.7 per animal, respectively; P < 0.01; Fig. 4A). Furthermore, ESM seemed to protect the oocyte against degeneration, which started on day 20. In ESM, more than 90% of the oocytes were alive at day 25, whereas fewer than 60% of the oocytes survived in GSM (P < 0.001; Fig. 4B). Even at day 40, more than 60% of the oocytes were alive in ESM (Fig. 4B).

Thus, oocytes growing under these conditions survived for 40 days in ESM, but they remained the size they had reached on day 16 (around 35 μm diameter). We then tested whether other factors promoted oocyte growth. Oocytes that had been cultured in GSM containing 50 ng/ml SCF for 10 days were cultured for 10 days more in the presence of serum and/or thecal cells. As shown in Figure 4C, both serum and thecal cells had significant effects on oocyte development (P < 0.001), increasing their mean diameter to about 45 μm. Figure 5A shows a group of oocytes developing in the presence of thecal stem cell colonies in ESM. The combination of thecal cells and serum further accelerated the development of the oocytes to about 50 μm in diameter (Fig. 4C). During prolonged culture with serum and thecal cells (32 days in total), some oocytes reached around 70 μm (Fig. 5B), which is similar to that of fully grown oocytes in antral follicles *in vivo*.

Fusing capacity of oocytes growing in vitro

To test the capacity of oocytes growing *in vitro* to fuse with spermatozoa, an *in vitro* fertilization assay was performed using capacitated spermatozoa. ZP-free oocytes that had developed for 21 days in either GSM or ESM in the presence of SCF were treated with Hoechst 33342, washed, and then inseminated. More

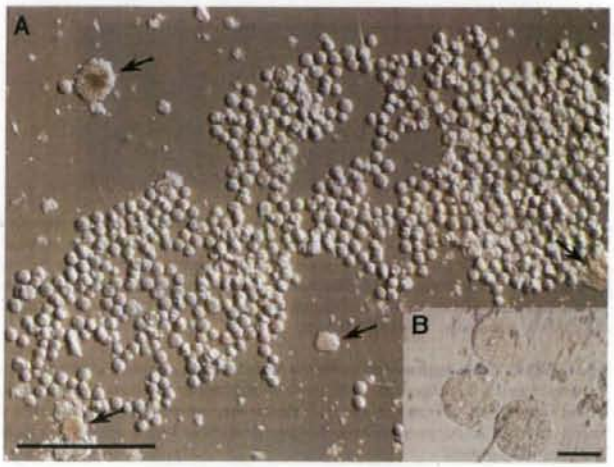

Fig. 5. Oocytes in the late growth phase. (A) *A group of oocytes developing* in vitro *in the presence of thecal stem cell colonies (arrows) after 20 days in embryonic stem cell medium (ESM). Most oocytes were still alive without the need for the support of granulosa cells. Scale bar: 500 μm.* **(B)** *Oocytes reaching their maximum normal size (around 70 μm) after 30 days of coculture with thecal cells in serum-containing EMS. Scale bar: 50 μm.*

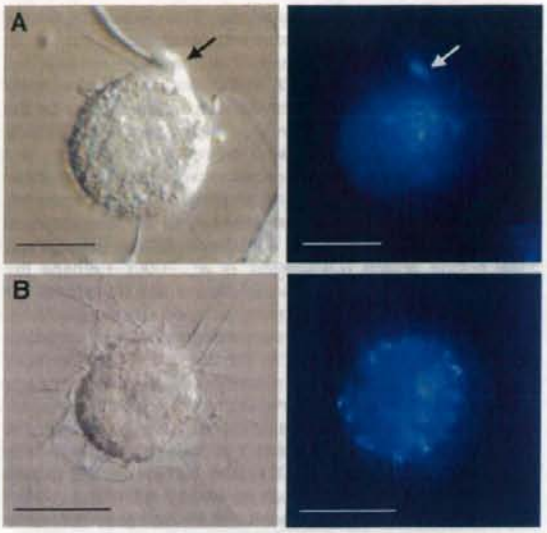

Fig. 6. Assessment of the fusion capacity of oocytes growing *in vitro*. *Both small* **(A)** *and large* **(B)** *oocytes could fuse with spermatozoa, observed as the transfer of Hoechst dye from the ooplasm to the sperm nucleus. The smaller oocyte shows a fertilization cone (arrow), normally found in fertilized oocytes. Scale bars: 20 μm (A) and 50 μm (B).*

than 70% of the oocytes examined had fused with the spermatozoa, as demonstrated by the transfer of the fluorescent dye to the sperm nucleus (Fig. 6A, B). Some oocytes showed fertilization cones in which a sperm head could be seen (Fig. 6A).

***Meiotic resumption by oocytes growing* in vitro**

The nucleolar configurations of the oocytes were visualized with Hoechst 33342 staining after sequential treatment with N6,O2-dibutyryl adenosine-3',5' cyclic-monophosphate (dbcAMP) and okadaic acid, as reported by Chesnel *et al.* (1994). About 10% of the oocytes had a bright ring around the nucleolus of their germinal vesicles (Fig. 7A). Such oocytes are the so-called "surrounded nucleolus" (SN) type, and are usually deemed to be oocytes with a higher capacity to undergo meiosis and develop into blastocysts (Zuccotti *et al.*, 2002). After a further 24 hours in culture, some (7/140) oocytes had entered metaphase I, with their condensed chromosomes aligned on the metaphase plate clearly visible with aceto-orcein staining (Fig. 7C). The remaining oocytes had no dye-positive ring around the nucleolus: the so-called "nonsurrounded nucleolus" (NSN) type (Fig. 7B). We found that okadaic acid treatment alone could also induce meiosis, but no SN-type oocytes were observed.

***Methylation status of imprinted genes in oocytes growing* in vitro**

Three groups of oocytes of different sizes (30–40 μm, 40–50 μm, and 50–60 μm) were subjected to DNA methylation analysis of the differentially methylated regions (DMRs) of Igf2r and Zac1 (maternally imprinted genes) and H19 (paternally imprinted gene). The results clearly showed that oocyte-size-dependent methylation progressed correctly in the two maternally imprinted genes (Igf2r and Zac1), with 73% and 80% of CpG regions methylated, respectively, in oocytes with 50–60 μm diameters (Fig. 8). The paternally imprinted gene, H19, remained unmethylated. This oocyte-size-dependent methylation imposition pattern was similar to that found in oocytes growing *in vivo* (Supplementary Fig. 2).

Discussion

This study demonstrates that the large-scale culture of growing oocytes from mouse neonatal ovaries is possible without the need for follicular cell support. The protocol optimized in this study for the preparation and culture of growing oocytes is shown in Figure 9, together with the developmental parameters of the oocytes. This finding is intriguing because it has been broadly accepted that follicle cells—especially granulosa cells—are the key modulators of growing oocytes and are indispensable for oocyte growth *in vitro* (Eppig *et al.*, 2002; Klinger and De Felici, 2002; van den Hurk and Zhao, 2005). Furthermore, as many as 800 growing oocytes per animal could be recruited from the resting pool of primordial oocytes using this culture system. Primordial follicles in neonatal ovaries are usually very difficult to collect intact; their follicular structure is very fragile. We surmise that the keys to success in this study included the less harmful method of oocyte collection and the use of a sequential culture system, which provided essential nutrients and growth factors while preventing the apoptosis that occurs normally in most growing oocytes *in vivo*.

The oocyte collection method we used was a modification of that developed for the isolation of thecal stem cells (Honda *et al.*, 2007). By selective culture with a serum-free medium, granulosa cells were effectively depleted from the ovarian cell suspension, together with other adhesive cells, such as fibroblast cells, as

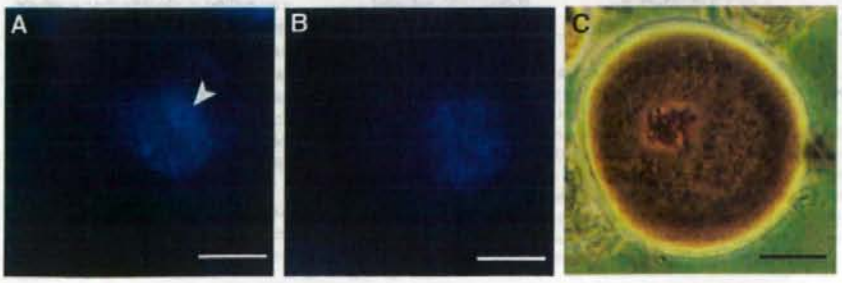

Fig. 7. Oocytes after sequential treatment with dbcAMP and okadaic acid. (A) *Some oocytes formed a Hoechst-positive bright ring around the nucleolus of the germinal vesicle (SN type; arrowhead).* **(B)** *The remaining oocytes had no bright ring around the nucleolus (NSN type).* **(C)** *Oocytes at meiosis I, with completely condensed chromosomes. Scale bars: 20 μm.*

confirmed by polymerase chain reaction (PCR) using specific primers (Honda *et al.*, 2007). The oocytes freed from the colonies continued to grow, like those recruited into the growing follicle pool *in vivo*, but without any supporting somatic cells. The culture system used in this study substituted—at least in part—for the somatic-cell-derived factors that normally support the growing oocytes. One of the factors that had a profound effect was SCF (Kit ligand), which also played an important role in the derivation of the oocytes from the thecal cell colonies. SCF is secreted from granulosa cells and acts on the oocyte via the Kit receptor on the oocyte membrane (Hutt *et al.*, 2006). This ligand–receptor interaction activates the PI3K–Akt pathway, which acts as an intraoocyte network for oogenesis in two ways: stimulating growth, while protecting against apoptosis (Liu *et al.*, 2006). This was also true for the action of SCF *in vitro*, because it produced dose-dependent increases in oocyte size and in the numbers of surviving oocytes. We confirmed that Kit receptors were correctly expressed at both the mRNA and protein levels (Fig. 3). We postulate that the lack of granulosa cells might have also contributed to the survival of the growing oocytes. Fas, a cell-surface receptor molecule that mediates apoptosis, is expressed on granulosa cells and induces follicular atresia, permitting fewer than 1% of follicles to develop (Sakamaki *et al.*, 1997). Recently, $p27^{kip1}$ has been identified as another apoptotic inducer expressed in granulosa cells in developing follicles (Rajareddy *et al.*, 2007). Thus, the lack of granulosa cells might have allowed the growing oocytes to escape follicular atresia.

As mentioned above, the oocytes stopped developing on day 20 in culture and initiated apoptosis. This pattern of oocyte development and degeneration *in vitro* (illustrated in Fig. 2A, B) may indicate that the requirements for oocyte growth are switched at some time around day 20. Within normal follicles, many nutrients and regulatory factors are supplied to oocytes by the surrounding granulosa cells in a paracrine fashion or directly through the gap junction network shared by the oocytes and granulosa cells. According to a gene knockout study that inhibited gap junction formation by the deletion of Gja4 (the gene encoding connexin 37), gap junctions are necessary for the progression to the preantral follicle stage, but not for early folliculogenesis and initial oocyte growth (Carabatsos *et al.*, 2000). Perhaps the oocyte growth arrest we observed around day 20 reflects the increasing dependency of growing oocytes on gap junctions. Interestingly, we found that this oocyte degeneration by apoptosis was ameliorated considerably by the use of ESM as the basic medium. ESM is a medium formulated for the establishment and maintenance of mouse embryonic stem cells and contains leukemia inhibitory factor (LIF) as its sole growth factor. By contrast, the GSM we initially used was developed for male germline stem cells (Kanatsu-Shinohara *et al.*, 2003) and contains many growth factors. Small metabolites, such as energy substrates, nucleotides, and amino acids, are transferred through gap junctions to growing oocytes (Eppig *et al.*, 2005). The composition of the ESM medium was possibly better suited to supply these small molecules to the naked oocytes in our culture system.

Besides oocyte survival, another important goal during oocyte growth *in vitro* is to attain a meiotically competent size (around 70 μm in diameter). The use of ESM as the basic medium significantly improved the survival of the oocytes, but did not further increase their size. This obstacle was overcome by the addition of serum to the medium or by coculture with thecal stem cells. We have not determined the optimal concentration of serum or the optimal density of thecal cells for this culture system. However, these two treatments seemed to act synergistically on oogenesis because the best result, in terms of the size of oocytes (50 μm mean diameter at day 25), was obtained when they were cultured in the presence of both factors. It will be interesting to identify the paracrine factors that are secreted from thecal cells to stimulate oocyte growth, because thecal cells are generally thought to supply steroid hormone sources or keratinocyte growth factors (Kezele *et al.*, 2005).

Normally, as oocytes grow in follicles, they undergo a series of nuclear and cytoplasmic modifications necessary for final oocyte

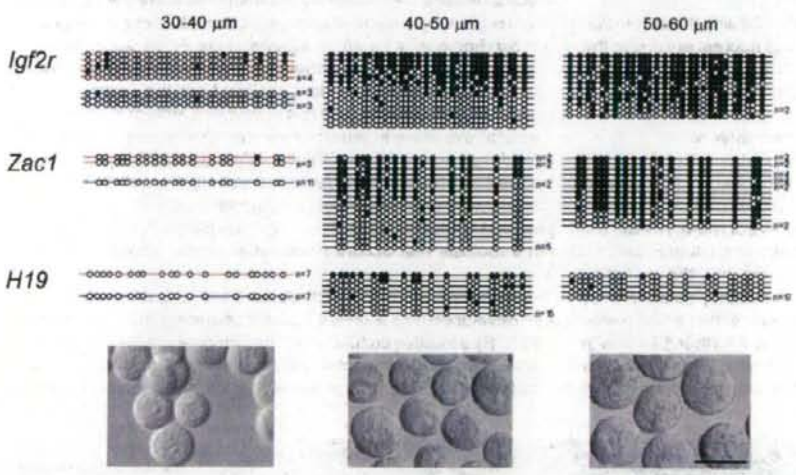

Fig. 8. The methylation status of the differentially methylated regions of three imprinted genes, *Igf2r*, *Zac1*, and *H19*, in three oocyte groups of different sizes. *Each horizontal line indicates the sequence from a single clone if the number of clones is not indicated. Open circles represent unmethylated CpG sequences and filled circles indicate methylated CpGs. Because the oocytes with 30–40 μm diameters were derived from (B6 X JF1) strain mice and had allelic polymorphisms, the maternal and paternal alleles are indicated by red and blue lines, respectively. The methylation patterns of the two maternally imprinted genes,* Igf2r *and* Zac1, *suggest that genomic imprinting was established in an oocyte-size-dependent manner. These methylation patterns are very similar to those of oocytes grown in vivo (see Supplementary Fig. 2). The paternally imprinted gene* H19 *remained unmethylated, irrespective of the size of the oocyte. Representative photographs of each oocyte group are shown at the bottom. Scale bars: 50 μm.*

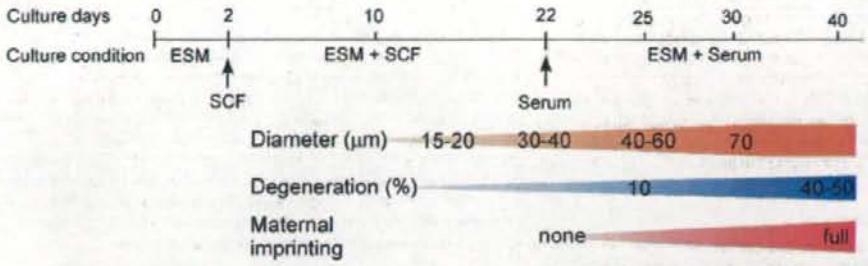

Fig. 9. Schematic diagram of the follicle-free *in vitro* oocyte growth system optimized in this study. *The protocol includes the use of embryonic stem cell medium (ESM) as the basal medium and treatment with stem cell factor (SCF) during the first half of culture, followed by treatment with serum in the second half of culture. As mentioned in the text, coculture with thecal stem cells was also beneficial for oocyte growth. The corresponding features of the developing oocytes are indicated.*

maturation and fertilization and for subsequent embryonic development. Our next undertaking was to determine whether oocytes growing *in vitro* showed signs of such developmental competence based on an autonomous program without supporting somatic cells. First, we examined the capacity of the oocytes to fuse with spermatozoa, using an *in vitro* fertilization assay. Within the ovary, growing oocytes become capable of fusion with spermatozoa as soon as they reach about 20 μm in diameter (Zuccotti *et al.*, 1994). Therefore, because it was very probable that growing oocytes could fuse with spermatozoa shortly after the initiation of culture, we examined whether the oocytes growing alone in culture retained their fusion capacity. Our result clearly indicated that the majority of oocytes retained this capacity even after 21 days in culture. Second, we tested whether oocytes growing *in vitro* resumed meiosis and entered metaphase. Some of the oocytes that had grown for 26 days in culture underwent germinal vesicle breakdown (GVBD) and complete chromosomal condensation after treatment with okadaic acid, an inhibitor of phosphatases 1A and 2A. This finding suggests that the oocytes might have accumulated the factors (e.g., p34cd2, cyclin B1, and cdc25; Kanatsu-Shinohara *et al.*, 2000) required for proceeding to metaphase I. Following treatment with dbcAMP, the nuclei of some oocytes showed a ring of Hoechst 33342-positive chromatin around the nucleolus (Fig. 7A). This SN nucleolar configuration appears in a subpopulation of oocytes *in vivo* and correlates well with meiotic competence and embryonic development (Zuccotti *et al.*, 2002; Inoue *et al.*, 2007). Because a high level of cAMP is supplemented by the surrounding granulosa cells through gap junctions (van den Hurk and Zhao, 2005), this dbcAMP treatment might have improved the quality of the granulosa-free oocytes. Thus, we succeeded in reproducing this process in oocytes growing *in vitro* to the metaphase I stage, although they did not complete meiosis to metaphase II. In this study, however, the proportion of oocytes reaching metaphase I (5%) was still lower than that of oocytes cultured with granulosa cells (35/150, 23 %; Klinger and de Felici, 2002). It is probable that the acquisition of meiotic competence by growing oocytes is highly dependent on the accompanying granulosa cells and that improvements in somatic-cell-free culture conditions are still required for the efficient derivation of meiosis-competent oocytes *in vitro*.

Finally, we examined whether maternal genomic imprinting was correctly imposed on the genomes of the growing oocytes. Without these maternal gene imprints, mammalian embryos cannot survive to term, as clearly demonstrated by the nuclear exchange experiments of Kono *et al.* (2002, 2004). The maternal imprint is imposed sequentially on the oocyte genome in an oocyte-size-dependent manner (Hiura *et al.*, 2006). Our DNA methylation analysis of two imprinted genes in growing oocytes of different diameters showed a correct size-dependent methylation pattern. This result has important implications for biology in that mammalian maternal genomic imprinting was established in these oocytes autonomously, independent of the follicular environment.

The application of technology to the growth and maturation of oocytes from the most abundant primordial follicles holds many attractions for clinical practice, animal production technology, and research. The somatic-cell-free culture system we have developed allows precise biochemical analyses, which are usually difficult to perform in the presence of somatic cell contaminants. Indeed, we could readily obtain data on the imprinting status of the growing oocytes, which usually requires laborious work to remove the surrounding granulosa cells. We also expect that some unknown oogenesis-related proteins (e.g., sperm–egg fusion proteins) might now be identified, because they can be purified efficiently from a bulk culture of growing oocytes. Furthermore, the information obtained under different culture conditions may lead to a better understanding of the mechanisms underlying oogenesis and offer some clues to the development of new systems of efficient oocyte production *in vitro*.

Materials and Methods

Cell preparation and culture

About 20 ovaries of newborn pups (2–4 days after birth) were obtained from ICR, C57BL/6 (B6), or hybrid B6 (Mus musculus musculus) X JF1 (Mus musculus molossinus) F1 mice. Cell culture was initiated according to a protocol for the establishment of putative thecal stem cells, which was modified from a protocol for the establishment of male germline stem cells (Kanatsu-Shinohara *et al.*, 2003; Honda *et al.*, 2007). In brief, isolated ovaries were treated with 1 mg/ml collagenase in Hanks's solution at 37 °C for 15 minutes and then treated with 0.2% trypsin and 1.4 mg/ml DNase for 10 minutes. Loosened ovarian tissues were dissected into single cells by gentle pipetting and were allocated to 6–8 wells of a 0.1% (w/v) gelatin-coated 24-well tissue culture plate (2.0–2.5 X 105 cells/well). The culture medium was essentially serum-free GSM (Kanatsu-Shinohara *et al.*, 2003). For the primary cell preparation, fibroblast cells were allowed to attach to the bottom of a gelatin-coated culture plate, and only the floating cells were passaged to the secondary culture plate. These replated cells attached weakly to the bottom of the culture wells during overnight culture and formed round colonies consisting of putative thecal stem cells and primordial oocytes. In some experiments, ESM was used. This consists of Dulbecco's modified Eagle's medium (high-glucose DMEM; In vitrogen,

Carlsbad, CA, USA) containing 15% knockout serum replacement (KSR; Invitrogen), 10^3 U/ml murine LIF (ESGRO; Invitrogen), 2 mM L-glutamine, 100 nM 2-mercaptoethanol, and nonessential amino acids. The cells were maintained at 37 °C under 5% CO_2 in air. When serum-containing ESM was prepared, 15% KSR was replaced with 10% fetal bovine serum. Half the culture medium was replaced every 2–3 days in all cultures.

In another series of experiments, we prepared ovarian cell suspensions from female mice 4, 9, and 14 days after birth and compared the efficiencies of thecal cell colony formation and the production of growing oocytes *in vitro*.

In vitro *preparation of oocytes*

Two days after the initiation of ovarian cell culture, SCF (Chemicon, Temecula, CA, USA) was added to the cultures at various concentrations (0, 5, 10, 50, and 100 ng/ml) and for different periods (0–28 days). The numbers of growing oocytes per unit area or the total in each well were scored.

BrdU-incorporation assay

To detect DNA synthesis in the growing oocytes *in vitro*, 100 μM BrdU was dissolved in the medium at the initiation of culture and incubated for two days. The cells were gently washed and cultured for 10 days in the presence of 100 ng/ml SCF. The incorporation of BrdU was detected using the BrdU Labeling and Detection Kit I (Roche, Basel, Switzerland), according to the manufacturer's protocol.

Detection of apoptosis

Apoptosis was analyzed by TUNEL, using an *in situ* apoptosis detection kit (TaKaRa, Shiga, Japan) according to the manufacturer's protocol. Thirty days after the initiation of culture using ESM in the presence of thecal stem cells, the oocytes were collected, washed with phosphate-buffered saline (PBS), and then fixed in 4% paraformaldehyde/PBS at room temperature for 30 minutes. After the oocytes had been washed three times with PBS, they were treated with permeabilization buffer for 3 minutes on ice. After the oocytes had been washed three more times in PBS, they were incubated in TUNEL reaction mixture containing TdT and dUTP–fluorescein isothiocyanate (FITC) at 37 °C for 1 hour. After three washes with PBS, the oocytes were incubated in Hoechst 33342. TUNEL-positive oocytes were detected by their FITC signal under fluorescence microscopy.

Expression analysis of Kit receptors at the mRNA and protein levels

Kit gene expression and the localization of the Kit protein product on the oocyte surface were analyzed in oocytes growing *in vitro*. Using ISOGEN (Nippon Gene, Toyama, Japan), total RNA was extracted from growing oocytes after 18 days in culture, from isolated thecal stem cells, and from the ovaries and testes of 2–3-month-old ICR mice. First-strand cDNA was synthesized using a TaKaRa RNA PCR kit with an oligo(dT)–3' site adaptor primer. Synthesized cDNA was subjected to PCR using specific primers (Table 1). To localize the Kit receptors on the oocyte surface, growing oocytes that had been cultured in serum-containing ESM *in vitro* were treated with acidic Tyrode's solution and pipetted several times under a dissecting microscope until the ZP had dissolved (approximately 1 minutes). After the removal of the ZP, the denuded oocytes were washed five times with fresh ESM, and then incubated for 4 hours to allow the surface proteins to recover. The ZP-free oocytes were fixed in 4% paraformaldehyde/PBS at room temperature for 30 minutes. After the oocytes had been washed five times with PBS, they were incubated in 5% normal goat serum/PBS at room temperature for 1 hour to block any nonspecific antibody binding sites. The oocytes were then incubated overnight at 4 °C with polyclonal goat antibody raised against mouse Kit protein (sc-1494; Santa Cruz Biotechnology, Santa Cruz, CA, USA), and then washed five times in 1% bovine serum albumin/PBS. The oocytes were then exposed to secondary antibody (FITC-conjugated rabbit antigoat IgG; Sigma-Aldrich, St Louis, MO, USA) for 1 hour at room temperature. Oocytes exposed to normal goat serum and then to the secondary antibody were used as the control. The distribution of Kit protein was observed with a fluorescence microscope.

TABLE 1

PRIMER SETS FOR GENE EXPRESSION ANALYSIS

Gene	Forward primer	Reverse primer	Product size, bp
Zp1	5'-ccaatggccgtgtggal-3'	5'-ggtggtggggtgagaaga-3'	825
Mvh	5'-ggtccaaaagtgacatatatacco-3'	5'-ttggtgatcagttctcgagt-3'	399
Kit	5'-gatctgctctgcgtctgtt-3'	5'-ctgattgtgctggatggatg-3'	108
G3pdh	5'-gtgttcctaccccaatgtg-3'	5'-gtcattgagagcaatgccag-3'	214

Evaluation of the oocyte chromatin configuration as an index of meiosis resumption competence

Oocytes growing *in vitro* never entered metaphase I spontaneously, even after prolonged culture. Therefore, we treated these oocytes sequentially with dbcAMP and okadaic acid, which are known to induce GVBD in oocytes lacking spontaneous meiotic competence (Chesnel *et al.*, 1994; Klinger and De Felici, 2002). The oocytes that had been cultured in SCF-containing ESM for 21 days were treated with 200 μM dbcAMP in serum-containing ESM for three days. After the oocytes had been thoroughly washed and cultured in serum-containing ESM for 24 hours, they were treated with 1 μM okadaic acid in serum-containing ESM for 3 hours. They were then washed and further cultured in serum-containing ESM for 24 hours. At the end of the culture period, any meiotic resumption by the oocytes was evaluated by staining them with Hoechst 33342 to observe their nucleolar configuration. Some oocytes were selected randomly for whole-mount preparations. They were mounted and compressed between a slide glass and a coverslip, and then fixed with 2.5% glutaraldehyde in 0.1 M cacodylate buffer (pH 7.4) for 20 minutes. After the samples had been washed with distilled water and dehydrated with ethanol, they were stained with 1% aceto-orcein for 1–2 minutes and observed with a phase contrast microscope.

Sperm–oocyte fusion assay

Cauda epididymal sperm from ICR strain mice were dispersed in 400 μl drops of human tubal fluid (HTF) medium (Quinn *et al.*, 1985) and incubated at 37 °C under 5% CO_2 in air for 2 hours to induce the capacitation and spontaneous acrosome reactions. Growing oocytes were generated with GSM 20 days after the ovarian cell cultures had been treated with SCF and were transferred to 100 μl drops of HTF medium. After three washes with fresh HTF, the oocytes were transferred to HTF drops containing 5 μg/ml Hoechst 33342. They were incubated for a further 15 minutes and then washed four times with fresh HTF medium. To remove the ZP, the oocytes were incubated with acidic Tyrode's solution, as described above. The ZP-free oocytes were washed three times with fresh HTF medium and capacitated spermatozoa (150 sperm/μl) were added and incubated at 37 °C under 5% CO_2 in air for 30 minutes. The oocytes were then subjected to gentle pipetting to remove the loosely bound sperm, and were transferred to a drop of HTF/0.25% glutaraldehyde for fixation. To confirm sperm–oocyte fusion, fluorescence microscopy under UV excitation was used to detect the transfer of Hoechst 33342 from the oocyte to the sperm.

Analysis of genomic imprinting status

Genomic imprinting is erased during the development of primordial germ cells, and the maternal imprint is reestablished during postnatal oocyte growth (Reik and Walter, 2001). The maternal imprint is imposed sequentially on the oocyte genome as the DNA methylation of the DMRs of each imprinted gene in an oocyte-size-dependent manner (Hiura *et al.*, 2006). We examined whether the maternal imprint was established correctly in the genomes of oocytes growing *in vitro* without follicular support. Three groups of oocytes of different sizes (30–40 μm, 40–50 μm,

and 50–60 μm in diameter) were prepared for the analysis. The smallest group (30–40 μm) was collected from (B6 X JF1) F1 strain oocytes that had been cultured for 18 days in SCF-containing GSM. The remaining two size groups were collected from ICR strain oocytes that had been cultured for 10 days in GSM followed by 26 days in ESM containing serum. DNA was isolated and subjected to bisulfate-sequencing methylation analysis of the DMRs of the Igf2r, Zac1, and H19 genes, as described by Hiura *et al.* (2006). Oocytes growing *in vivo* were collected from juvenile B6D2F1 mice and used as the controls.

Statistical analysis

Mean values were compared using one-way ANOVA, following arcsine transformation if necessary. Where appropriate, the significance of differences among the means was determined with Scheffe's F test. $P < 0.05$ was considered significant. All experiments were replicated at least twice.

Acknowledgments

We thank Dr Yuji Hirao for his very helpful discussions and suggestions on oocyte survival and apoptosis. This research was supported by grants from MEXT (AH and AO), MHLW (AO), and CREST (AO). AH is the recipient of a research fellowship from the RIKEN Special Postdoctoral Researchers Program. The JF1 mice used in this study belong to Dr T. Shiroishi, National Institute of Genetics (Japan), and were provided by the RIKEN BioResource Center with the support of the National BioResources Project of MEXT, Japan.

References

BROWER, P. T. and SCHULTZ, R. M. (1982). Intercellular communication between granulosa cells and mouse oocytes: existence and possible nutritional role during oocyte growth. *Dev. Biol.* 90: 144–153.

CANNING, J., TAKAI, Y. and TILLY, J. L. (2003). Evidence for genetic modifiers of ovarian follicular endowment and development from studies of five inbred mouse strains. *Endocrinology* 144: 9–12.

CARABATSOS, M. J., SELLITTO, C., GOODENOUGH, D. A. and ALBERTINI, D. F. (2000). Oocyte–granulosa cell heterologous gap junctions are required for the coordination of nuclear and cytoplasmic meiotic competence. *Dev. Biol.* 226: 167–179.

CHESNEL, F., WIGGLESWORTH, K. and EPPIG, J. J. (1994). Acquisition of meiotic competence by denuded mouse oocytes: participation of somatic-cell product(s) and cAMP. *Dev. Biol.* 161: 285–295.

DE FELICI, M., KLINGER, F. G., FARINI, D., SCALDAFERRI, M. L., IONA, S. and LOBASCIO, M. (2005). Establishment of oocyte population in the fetal ovary: primordial germ cell proliferation and oocyte programmed cell death. *Reprod. Biomed. Online* 10: 182–191.

EPPIG, J. J. and O'BRIEN, M. J. (1996). Development *in vitro* of mouse oocytes from primordial follicles. *Biol. Reprod.* 54: 197–207.

EPPIG, J. J., WIGGLESWORTH, K. and PENDOLA, F. L. (2002). The mammalian oocyte orchestrates the rate of ovarian follicular development. *Proc. Natl Acad. Sci. USA* 99: 2890–2894.

EPPIG, J. J., PENDOLA, F. L., WIGGLESWORTH, K. and PENDOLA, J. K. (2005). Mouse oocytes regulate metabolic cooperativity between granulosa cells and oocytes: amino acid transport. *Biol. Reprod.* 73: 351–357.

HAGHIGHAT, N. and VAN WINKLE, L. J. (1990). Developmental change in follicular cell-enhanced amino acid uptake into mouse oocytes that depends on intact gap junctions and transport system. *J. Exp. Zool.* 253: 71–82.

HIRSHFIELD, A. N. (1991). Development of follicles in the mammalian ovary. *Int. Rev. Cytol.* 124, 43–101.

HIURA, H., OBATA, Y., KOMIYAMA, J., SHIRAI, M. and KONO, T. (2006). Oocyte growth-dependent progression of maternal imprinting in mice. *Genes Cells* 11: 353–361.

HONDA, A., HIROSE, M., HARA, K., MATOBA, S., INOUE, K., MIKI, H., HIURA, H., KANATSU-SHINOHARA, M., KANAI, Y., KONO, T., SHINOHARA, T. and OGURA, A. (2007). Isolation, characterization and *in vitro* and *in vivo* differentiation of putative thecal stem cells. *Proc. Natl Acad. Sci. USA* 104: 12389–12394.

HUTT, K. J., MCLAUGHLIN, E. A. and HOLLAND, M. K. (2006). Kit ligand and c-Kit have diverse roles during mammalian oogenesis and folliculogenesis. *Mol. Hum. Reprod.* 12: 61–69.

INOUE, A., AKIYAMA, T., NAGATA, M. and AOKI, F. (2007). The perivitelline space-forming capacity of mouse oocytes is associated with meiotic competence. *J. Reprod. Dev.* 53: 1043–1052.

JOHNSON, J., CANNING, J., KANEKO, T., PRU, J. K. and TILLY, J. L. (2004). Germline stem cells and follicular renewal in the postnatal mammalian ovary. *Nature* 428: 145–150.

KANATSU-SHINOHARA, M., SCHULTZ, R. M. and KOPF, G. S. (2000). Acquisition of meiotic competence in mouse oocytes: absolute amounts of p34(cdc2), cyclin B1, cdc25C and wee1 in meiotically incompetent and competent oocytes. *Biol. Reprod.* 63: 1610–1616.

KANATSU-SHINOHARA, M., OGONUKI, N., INOUE, K., MIKI, H., OGURA, A., TOYOKUNI, S. and SHINOHARA, T. (2003). Long-term proliferation in culture and germline transmission of mouse male germline stem cells. *Biol. Reprod.* 69: 612–616.

KEZELE, P., NILSSON, E. E. and SKINNER, M. K. (2005). Keratinocyte growth factor acts as a mesenchymal factor that promotes ovarian primordial to primary follicle transition. *Biol. Reprod.* 73: 967–973.

KLINGER, F. G. and DE FELICI, M. (2002). *In vitro* development of growing oocytes from fetal mouse oocytes: stage-specific regulation by stem cell factor and granulosa cells. *Dev. Biol.* 244: 85–95.

KONO, T., SOTOMARU, Y., KATSUZAWA, Y. and DANDOLO, L. (2002). Mouse parthenogenetic embryos with monoallelic *H19* expression can develop to day 17.5 of gestation. *Dev. Biol.* 243: 294–300.

KONO, T., OBATA, Y., WU, Q., NIWA, K., ONO, Y., YAMAMOTO, Y., PARK, E. S., SEO, J. S. and OGAWA, H. (2004). Birth of parthenogenetic mice that can develop to adulthood. *Nature* 428: 860–864.

LIU, K., RAJAREDDY, S., LIU, L., JAGARLAMUDI, K., BOMAN, K., SELSTAM, G. and REDDY, P. (2006). Control of mammalian oocyte growth and early follicular development by the oocyte PI3 kinase pathway: new roles for an old timer. *Dev. Biol.* 299: 1–11.

OBATA, Y. and KONO, T. (2002). Maternal primary imprinting is established at a specific time for each gene throughout oocyte growth. *J. Biol. Chem.* 277: 5285–5289.

PEPLING, M. E. and SPRADLING, A. C. (2001). Mouse ovarian germ cell cysts undergo programmed breakdown to form primordial follicles. *Dev. Biol.* 234: 339–351.

QUINN, P., KERIN, J. F. and WARNES, G. M. (1985). Improved pregnancy rate in human *in vitro* fertilization with the use of a medium based on the composition of human tubal fluid. *Fertil. Steril.* 44: 493–498.

RAJAREDDY, S., REDDY, P., DU, C., LIU, L., JAGARLAMUDI, K., TANG, W., SHEN, Y., BERTHET, C., PENG, S. L., KALDIS, P. and LIU, K. (2007). p27kip1 (Cdkn1b) controls ovarian development by suppressing follicle endowment and activation and promoting follicle atresia in mice. *Mol. Endocrinol.* 21: 2189–2202.

REIK, W. and WALTER, J. (2001). Genomic imprinting: parental influence on the genome. *Nat. Rev. Genet.* 2: 21–32.

SAKAMAKI, K., YOSHIDA, H., NISHIMURA, Y., NISHIKAWA, S. and MANABE, N., YONEHARA, S. (1997). Involvement of Fas antigen in ovarian follicular atresia and luteolysis. *Mol. Reprod. Dev.* 47: 11–18.

VAN DEN HURK, R. and ZHAO, J. (2005). Formation of mammalian oocytes and their growth, differentiation and maturation within ovarian follicles. *Theriogenology* 63: 1717–1751.

ZUCCOTTI, M., PICCINELLI, A., MARZILIANO, N., MASCHERETTI, S. and REDI, C. A. (1994). Development and loss of the ability of mouse oolemma to fuse with spermatozoa. *Zygote* 2: 333–339.

ZUCCOTTI, M., PONCE, R. H., BOIANI, M., GUIZZARDI, S., GOVONI, P., SCANDROGLIO, R., GARAGNA, S. and REDI, C. A. (2002). The analysis of chromatin organization allows selection of mouse antral oocytes competent for development to blastocyst. *Zygote* 10: 73–78.

J. ID: Z8T Customer A. ID: 2008-0113.R1 Cadmus Art: DVG20451 Date: 20-NOVEMBER-08 Stage: I Page: 1

© 2008 Wiley-Liss, Inc.

genesis 00:000–000 (2008)

TECHNOLOGY REPORT

Efficient Production of Androgenetic Embryos by Round Spermatid Injection

Hiromi Miki,[1] Michiko Hirose,[1] Narumi Ogonuki,[1] Kimiko Inoue,[1,2] Fuyuko Kezuka,[1] Arata Honda,[1] Kazuyuki Mekada,[1] Ken-Ichi Hanaki,[3] Hirotaka Iwafune,[4] Atsushi Yoshiki,[1] Fumitoshi Ishino,[4] and Atsuo Ogura[1,2,3]*

[1]RIKEN Bioresource Center, Tsukuba, Ibaraki, Japan
[2]Graduate School of Life and Environmental Science, University of Tsukuba, Tsukuba, Ibaraki, Japan
[3]The Center for Disease Biology and Integrative Medicine, Faculty of Medicine, University of Tokyo, Bunkyo-ku, Tokyo, Japan
[4]Medical Research Institute, Tokyo Medical and Dental University, Chiyoda-ku, Tokyo, Japan

Received 10 August 2008; Revised 16 September 2008; Accepted 21 September 2008

Summary: Mammalian androgenetic embryos can be produced by pronuclear exchange of fertilized oocytes or by dispermic in vitro fertilization of enucleated oocytes. Here, we report a new technique for producing mouse androgenetic embryos by injection of two round spermatid nuclei into oocytes, followed by female chromosome removal. We found that injection of round spermatids resulted in high rates of oocyte survival (88%). Androgenetic embryos thus produced developed into mid-gestation fetuses at various rates, depending on the mouse strain used. All the fetuses examined maintained paternally specific genomic imprinting memories. This technique also enabled us to produce complete heterozygous F1 embryos by injecting two spermatids from different strains. The best rate of fetal survival (12% per embryos transferred) was obtained with C57BL/6 × DBA/2 androgenetic embryos. We also generated embryonic stem cell lines efficiently with the genotype of *Mus musculus domesticus* × *M. m. molossinus*. Thus, injection of two round spermatid nuclei followed by maternal enucleation is an effective alternative method of producing androgenetic embryos that consistently develop into blastocysts and mid-gestation fetuses. genesis 00:000–000, 2008. © 2008 Wiley-Liss, Inc.

Key words: oocyte; ICSI; ROSI; androgenesis; fetus; embryo

Androgenic and parthenogenetic embryos, having uniparental genomes, are very useful models for the study of parental specific gene expression or for discovering imprinted genes (Kaneko-Ishino *et al.*, 2003). Diploid parthenogenetic embryos can be produced conventionally by repression of second polar body formation, whereas diploid androgenic embryos have been constructed in several ways, each of which needs micromanipulation procedures and some technical skills. Since the first demonstration of their limited and characteristic postimplantation development more than 20 years ago, androgenic embryos have been produced usually by pronuclear transplantation between two zygotes (Barton *et al.*, 1984; McGrath and Solter, 1984; Surani *et al.*, 1984). More recently, Obata *et al.* (2000) developed a new technique consisting of enucleation of oocytes followed by in vitro fertilization (IVF), which allows penetration of two spermatozoa (dispermic fertilization). This protocol was highly efficient in production of diploid androgenic embryos, and the androgenic embryos thus produced showed very good developmental rates to blastocysts. However, the optimization of conditions for achieving polyspermic IVF can vary with the strain of spermatozoa used, and the technique might not be applicable to spermatozoa from inbred strains with low inherent fertilization ability. This study was undertaken to determine whether direct injection of two male germ cell nuclei into oocytes could be used for the construction of androgenetic embryos.

In a preliminary study, we constructed diploid androgenetic embryos by injecting two sperm nuclei into enucleated oocytes simultaneously. However, the proportions of oocytes surviving the injection were extremely low (<30%) because this approach resulted in the influx of a large amount of the medium into the oocytes and because enucleation before injection weakened the oocytes significantly. Therefore, we used injection first, followed by removal of the female chromo-

Additional Supporting Information may be found in the online version of this article.

*Correspondence to: Atsuo Ogura, RIKEN Bioresource Center, Tsukuba, Ibaraki 305-0074, Japan.
E-mail: ogura@rtc.riken.go.jp

Contract grant sponsor: KAKENHI; Contract grant numbers: 20062012, 19300151, 19880037

Published online 00 Month 2008 in Wiley InterScience (www.interscience.wiley.com)
DOI: 10.1002/dvg.20451

ID: viiavk Date: 20/11/08 Time: 20:21 Path: J:/Production/DVG#/Vol00000/080102/3B2/C2DVG#080102

J. ID: Z8T Customer A. ID: 2008-0113.R1 Cadmus Art: DVG20451 Date: 20-NOVEMBER-08 Stage: I Page: 2

somes from the oocytes. The female chromosomes could be easily removed from sperm-activating oocytes, together with the second polar body. We also examined the effectiveness of injection of two round spermatids, instead of mature sperm heads, because smaller injection pipettes can be used for these small cells, and this helps to minimize the damage to recipient oocytes (about 3.5 μm vs. 5.0 μm for sperm injection). Round spermatids were injected into oocytes, which had been activated with strontium treatment. As expected, the use of intact oocytes for sperm injection increased the oocyte survival rate to 65.3%, and the rate was further improved to 88.3% by round spermatids injection ($P < 0.05$; Table 1). Therefore, for the next series of experiments, we employed the protocol of injection of two round spermatid nuclei into a preactivated oocyte followed by female chromosome removal (Fig. 1a). T1 F1

Table 1
Survival of Oocytes After Injection of Round Spermatids or Sperm Into B6D2F1 Oocytes

Male germ cell nucleus	Oocyte	No. injected	No. of survived (%)	
Two round spermatid nuclei	Activated	197	174	(88.3)[a]
Two sperm nuclei	MII	49	32	(65.3)[a]
One round spermatid nucleus	Activated	100	91	(91.0)
One sperm nucleus	MII	39	31	(79.5)

[a]$P < 0.001$(Fisher's exact probability test).

To analyze the developmental ability of diploid androgenetic embryos constructed with two round spermatid nuclei, embryos that reached the two-cell stage were transferred into the oviducts of pseudopregnant recipient females, and their uteri were examined at 9.5 days post coitus (dpc). Irrespective of the strains used for the paternal genome or ooplasm, a proportion of the embryos underwent implantation and developed into fetuses (Fig. 1b), although development of the embryos constructed from the JF1 genome was poor (Table 2). As T2

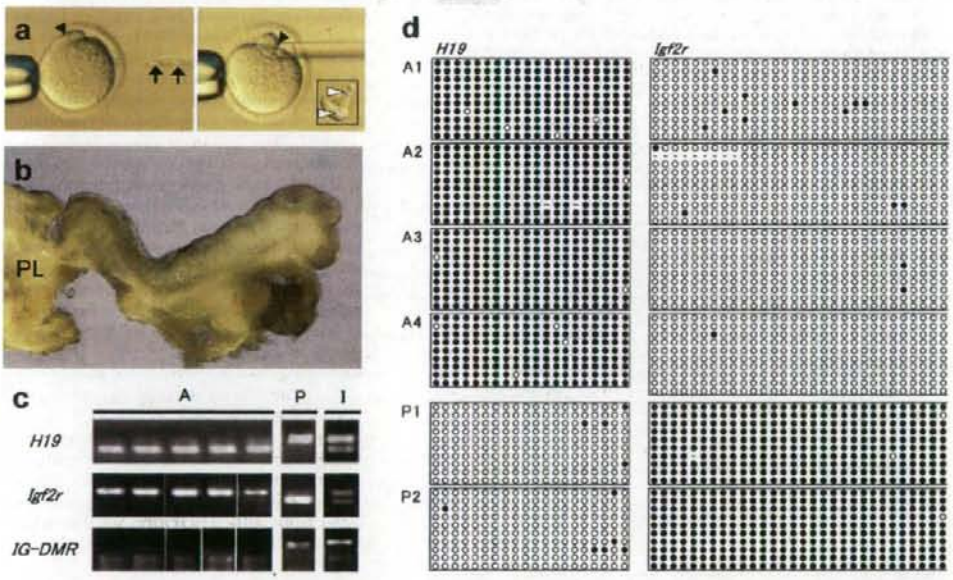

COLOR

FIG. 1. Reconstruction of an androgenetic embryo and the imprinting status of resulting androgenetic fetuses. (**a**) (Left) Two round spermatid nuclei (arrows) are injected into a preactivated oocyte with a semiprotruded second polar body (arrowhead). (Right) A few hours later, the female chromosomes are removed together with the second polar body (arrowhead). A removed karyoplast contains two chromosomal masses: one from the second polar body and one from the ooplasm (Hoechst stained, arrowheads in inset). (**b**) A typical E9.5 androgenetic fetus derived from injection of two round spermatid nuclei. PL, placenta. (**c**) DNA methylation status of imprinted genes, *Igf2r* and *IG-DMR* in E9.5 fetuses demonstrated by COBRA. Androgenetic fetuses (A) exclusively show the paternally imprinted pattern. P, parthenogenetic fetuses; I, ICSI-generated fetus. (**d**) DNA methylation status of the differentially methylated regions (DMRs) of *H19* and *Igf2r* demonstrated by bisulfite sequence. Hypermethylation of a paternally imprinted DMR (*H19*) and hypomethylation of a maternally imprinted DMR (*Igf2r*) are shown for androgenetic fetuses (A1–A4) and vice versa for parthenogenetic fetuses (P1 and P2). Open circles and filled circles indicate unmethylated and methylated CpG sequences, respectively. AQ2

ID: vilavk Date: 20/11/08 Time: 20:21 Path: J:/Production/DVG#/Vol00000/080102/3B2/C2DVG#080102

J. ID: Z8T Customer A. ID: 2008-0113.R1 Cadmus Art: DVG20451 Date: 20-NOVEMBER-08 Stage: I Page: 3

Table 2
Development In Vitro and In Vivo of Androgenetic Embryos from Different Strains of Oocytes and Round Spermatids

Strain of oocyte	Strain of round spermatid	No. of experiment	No. cleaved/ cultured (%)		No. of embryos transferred	No. implanted (% transferred)		No. of surviving fetuses at 9.5 dpc (normal, retarded) (% transferred)	
B6D2F1	B6D2F1 × B6D2F1	3	117/155	(75.4)	111	30	(27.0)	7 (5, 2)	(7.7)
B6D2F1	B6 × DBA2	2	92/130	(70.7)	92	38	(41.3)	11 (9, 2)	(12.0)
B6D2F1	129 × 129	7	297/499	(59.4)	320	55	(17.2)	11 (10, 1)	(6.6)
B6D2F1	JF1 × JF1	8	516/854	(60.4)	534	110	(20.6)	1 (0, 1)	(0.2)
129	B6D2F1 × B6D2F1	3	66/152	(43.4)	66	11	(16.7)	4 (4, 0)	(7.3)
129	129 × 129	4	130/238	(54.6)	130	26	(20.0)	5 (3, 2)	(3.8)

Table 3
Complete Heterozygocity in B6 × DBA/2 Androgenetic Fetuses Confirmed by Polymorphisms of 12 Microsatellite Markers A–L

Strain of round spermatids	No. of fetuses	% heterogygous between B6 and DBA/2											
		A	B	C	D	E	F	G	H	I	J	K	L
B6 × DBA/2	11	100	100	100	100	100	100	100	100	100	100	100	100
B6D2F1 × B6D2F1	8	50.0	62.5	75.0	50.0	37.5	37.5	50.0	50.0	25.0	50.0	75.0	37.5

far as we examined, all fetuses maintained their expected DNA methylation patterns for three paternally imprinted regions, *H19*, *IG-DMR*, and *Igf2r* (Fig. 1c,d). The androgenetic fetuses obtained from round spermatid injection were morphologically indistinguishable from those obtained from mature spermatozoa, as described earlier (Obata *et al.*, 2000; Surani *et al.*, 1984) (Fig. 1b).

The best rate of development to fetuses was obtained when two round spermatids each from the C57BL/6 (B6) or DBA/2 (D2) strains were coinjected into oocytes (about 12% per transfer; Table 2). Theoretically, the use of hybrid F1 male gametes (e.g., B6D2F1) for androgenesis does not necessarily result in reconstruction of the complete hybrid genome in embryos, because two sets of chromosomes are segregated randomly at the first meiotic division before haploidization. In contrast, coinjection of two haploid male gametes from different inbred strains always results in production of the complete hybrid set of chromosomes. To confirm this assumption, we analyzed the genotype of fetuses from the B6 × D2 group and the B6D2F1 × B6D2F1 group using 12 polymorphic markers identifying the B6 and D2 alleles. As expected, all markers were heterozygous in the former group whereas some markers were homozygous for either strain in the latter group (Table 3). It is T3 well known that hybrid vigor is manifested when embryos are manipulated in vitro, including simply in vitro culture (Suzuki *et al.*, 1996), microinsemination (Endoh *et al.*, 2007; Kawase *et al.*, 2001), and somatic cell nuclear transfer (Inoue *et al.*, 2003; Wakayama and Yanagimachi, 2001). Although not statistically significant, the highest developmental ability of embryos derived from B6 × D2 round spermatids might have been due to such complete hybrid genetic composition. In the case of parthenogenesis, complete hybrid genetic composition was achieved by transfer of a metaphase II karyoplast of one strain to an oocyte of another strain, which was then activated to restore diploidy (Hikichi *et al.*, 2007). Hybrid parthenogenetic ES cells were also generated from these embryos for polymorphic analysis, as in this study (below).

To exploit this technical advantage, we produced androgenetic embryos using round spermatids from B6 (*M. m. domesticus*) and JF1 (*M. m. molossinus*) and cultured them to the blastocyst stage to generate intersubspecies hybrid androgenetic embryonic stem (aES) cells. Of the 46 embryos constructed, 20 (43%) developed into blastocysts. Eight aES cell lines (40% of blastocysts) were generated under our conventional culture condition for fertilization-derived ES cells (Shinmen *et al.*, 2007). All lines showed high in vitro proliferation potential, a high alkaline phosphatase activity (Fig. 2a), and F2 the normal $2n = 40$ karyotype (Fig. 2b). Their hybrid F1 genetic composition was confirmed at least for two genes in all eight cell lines (Fig. 2c). Four were identified as XX androgenome genotype and four more as XY (Fig. 2d). No cell line with the YY type was found as in earlier report (Obata *et al.*, 2000). Randomly selected lines (#2, #3, and #4) were examined for embryoid body (EB) formation. Dissociated cells were cultured in the presence of serum under a feeder-cell-free condition. About 10 days later, EBs with a typical morphology were formed (Fig. 2e).

This study has demonstrated for the first time that the genome of round spermatids—the youngest stage of haploid male germ cells—scan support development of androgenetic embryos to the middle fetal stage as effectively as those reported for other methods of androgenesis using mature spermatozoa. Mouse embryos fertilized with a round spermatid maintained a normal genomic imprinting memory (Shamanski *et al.*, 1999), and the resultant offspring showed no abnormal phenotypes (Tamashiro *et al.*, 1999). By contrast, Kishigami *et al.* (2006) reported that the paternal zygotic genome derived from a round spermatid was abnormally remethylated follow-

ID: viiavk Date: 20/11/08 Time: 20:22 Path: J:/Production/DVG#/Vol00000/080102/3B2/C2DVG#080102

J. ID: Z8T Customer A. ID: 2008-0113.R1 Cadmus Art: DVG20451 Date: 20-NOVEMBER-08 Stage: I Page: 4

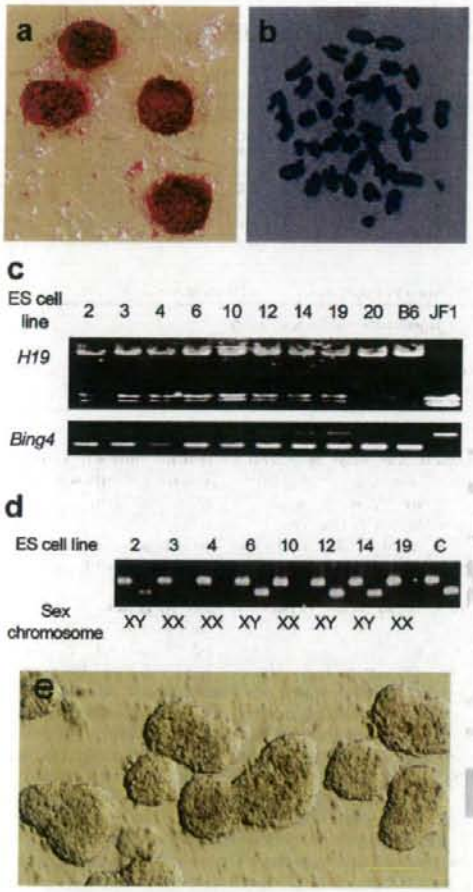

FIG. 2. Analyses of aES cell lines derived from B6 × JF1 androgenetic blastocysts. (**a**) ES cell colonies stained for alkaline phosphatase. All ($n = 8$) cell lines showed a high alkaline phosphatase activity. (**b**) A chromosome preparation of an ES cell. All androgenetic ES cell lines had the normal karyotype with 40 chromosomes. (**c**) Polymorphic analysis for the B6 × JF1 genome in androgenetic ES cell lines. Heterozygosity was confirmed for the two loci examined in all cell lines. #20, fertilization-derived male B6 ES cell line; (**d**) Sex chromosome compositions in aES cell lines. The X chromosomes were detected by the sequence for *Xist* (left lane) and the Y chromosomes by *Zfy* (right lane). Four lines were XX, and the remaining four lines were XY. No cell line with the YY type was found. C, a control male genome from a tail. (**e**) Typical EBs that developed from #3 aES cell line. Bar: 100 μm.

ing rapid demethylation at fertilization, although whether such epigenetic abnormality might affect subsequent embryonic and postnatal development remains to be determined. Therefore, we also tested whether the androgenetic fetuses we obtained were epigenetically equivalent to those obtained using mature sperm genomes, but the genomic imprinting as far as we examined was correctly maintained in these spermatid-derived fetuses. From the technical viewpoint, the only drawback associated with our androgenesis method would be the intracytoplasmic injection of mouse oocytes, which needs a high level of technical skill and experience because of the high sensitivity of mouse oocytes to puncturing. However, this technical difficulty can be easily overcome using Piezo-impact units, which have been extensively used for microassisted fertilization and nuclear transfer cloning in mice. Injection of round spermatid nuclei is easier than injection of mature sperm nuclei because they are malleable. Furthermore, activated oocytes are stronger than nonactivated oocytes against the injection stimulus, for unknown reasons. Thanks to these technical advantages, we found that about 80–100 androgenetic embryos could be produced per person in a single experiment. The existing androgenesis methods are reliable in many technical respects but not always suitable for the production of a large number of such embryos at one time. Our protocol is probably the most effective way to produce androgenetic embryos if the technique of intracytoplasmic injection of mouse oocytes is available.

METHODS

Mature metaphase II (MII) oocytes were collected from the oviducts of B6D2F1 or 129^{+tcr}/SvJcl female mice (Clea Japan, Japan) that were induced to superovulate with eCG and hCG. The oocytes were placed in KSOM medium (Lawitts and Biggers, 1993) and kept under 5% CO_2 in air at 37°C until use. Spermatogenic cells were isolated mechanically from the testes of male B6D2F1, 129^{+tcr}/SvJcl, C57BL/6Cr (B6), DBA/2 (D2) (SLC, Japan), or JF1 (RIKEN Bioresource Center) mice as described (Ogura and Yanagimachi, 1993). The cell suspension was washed by centrifugation (200*g*) and stored in GL-PBS medium (Ogura and Yanagimachi, 1993) at 4°C. Sperm masses were isolated from the cauda epididymis of B6D2F1 males, transferred to GL-PBS, and stored at room temperature until use.

Androgenic embryos were produced by round spermatid injection or intracytoplasmic sperm injection (ICSI) techniques. ICSI was performed according to Kimura and Yanagimachi (1995). To produce diploid androgenetic embryos using round spermatids, MII oocytes were preactivated by treatment with Ca^{2+}-free KSOM containing 2.5 mM $SrCl_2$ for 20 min. Two spermatid nuclei were injected into oocytes advancing to telophase II in Hepes-buffered KSOM at around 40–70 min after oocyte activation (Fig. 1a). The female nucleus was removed, together with the second polar body, within 4 h after oocyte activation in the presence of cytochalasin B (Calbiochem, San Diego, CA) as reported (Ogura *et al.*, 1999) (Fig. 1a).

ID: viiavk Date: 20/11/08 Time: 20:22 Path: J:/Production/DVG#/Vol00000/080102/3B2/C2DVG#080102

Most embryos that reached the two-cell stage within 24 h in culture were transferred into the oviducts of day 0.5 pseudopregnant ICR strain recipient females (Clea Japan, Japan). On day 9.5, the recipient females were sacrificed to collect fetuses (E9.5 fetus) for observation of their morphology and for genomic analyses.

For DNA methylation analysis of imprinting genes, genomic DNA from the fetuses was obtained by extraction with a lysis buffer containing 50 ng/ml proteinase K. After purification by phenol-chloroform extraction and ethanol precipitation, the DNA was used for combined bisulfite restriction enzyme analysis (COBRA) (Xiong and Laird, 1997) and bisulfite sequence as follows, respectively. For COBRA, genomic DNA was denatured in 10 μl of 0.2 M NaOH at 37°C for 15 min and treated with 140 μl of freshly prepared bisulfite solution [2.3 M sodium metabisulfite (Sigma-Aldrich, St. Louis, MO), 10 mM hydroquinone and 2 M NaOH] at 50°C for 4 h. The bisulfite-treated DNA was precipitated with isopropanol and sodium acetate, and desulfonated by treatment with 0.2 M NaOH for 15 min at 37°C. The bisulfite-converted DNA was precipitated by ethanol and ammonium acetate. Total DNA was amplified by polymerase chain reaction (PCR) for *H19* (Bartolomei *et al.*, 1991), *Igf2r* (Barlow *et al.*, 1991), and *IG-DMR* (Lin *et al.*, 2003) using Ex Taq HS (Takara, Otsu, Japan). The primer sequences and PCR conditions for the amplification of all target genes are provided in Supporting Information Table 1. The methylation states of the PCR products were confirmed by digestion with restriction enzymes that recognize methylated CpG sites: HPYCH4IV (New England Biolabs, Ipswich, MA) for *H19* and *IG-DMR*, and Taq1 (Fermentas, Hanover, MD) for *Igf2r*, respectively. The reaction products were separated electrophoretically on 2% agarose gels and stained with ethidium bromide. Signal intensities were measured using an image analyzer. For bisulfite sequencing, genomic DNA was treated with CpGenome DNA modification kits (Chemicon, Billerica, MA) according to the manufacturer's recommendations. The bisulfite-converted DNA was amplified by nested (or seminested) PCR using Ex Taq HS (Takara). Primer sequences and PCR conditions for the amplification of all target genes are given in Supporting Information Table 1. After amplification, the DNA fragments were separated by 2% agarose gel electrophoresis to purify the PCR products. The gels were stained with ethidium bromide, and the bands were excised and purified with Geneclean kits (MP Biochemicals, Irvine, CA) according to the manufacture instructions. These fragments were inserted into the plasmid vector pGEM-T Easy (Promega, Madison, WI) and transformed into ECOS competent *E. coli* (Nippon Gene, Tokyo, Japan). Isolated clones were purified using Labopass plasmid mini purification kits (Hokkaido System Science, Sapporo, Japan). DNA was sequenced using BigDye Terminator Cycle Sequencing Kit and analyzed using an ABI PRISM 3100 Genetic Analyzer (Applied Biosystems, Foster City, CA).

The E9.5 fetuses derived from B6 and D2 round spermatids were examined using simple sequence length polymorphism markers to distinguish between B6 and D2 alleles using PCR amplification. DNA was extracted using Wizard Genomic DNA Purification Kits (QIAGEN, Madison, WI) according to the manufacturer's recommendations. Twelve markers (D1Mit170, D1Mit155, D2Mit293, D2Mit456, D3Mit151, D3Mit147, D4Mit171, D4Mit234, D5Mit294, D5Mit161, D6Mit74, and D6Mit15) were amplified using a 2 × Qiagen Multiplex PCR Master Mix (QIAGEN) for 32 cycles of 94°C for 30 s, 60°C for 90 s, and 72°C for 30 s. After the reaction, the PCR products were applied to a 4% agarose gel and separated electrophoretically. The gels were stained with ethidium bromide to detect the PCR products.

Embryos derived from B6 and JF1 round spermatids were cultured in vitro for 96 h, and blastocysts were used for the establishment of ES cells as described (Shinmen *et al.*, 2007). Chromosome compositions, sex, and allelic polymorphisms were examined after feeder cells were removed by plating on a gelatin-coated dish for 30 min, twice. To evaluate chromosomes in aES cells, metaphase cells were prepared by treatment with 0.05 μg/ml Colcemid (Invitrogen, Carlsbad, CA) for 4–6 h. The cells were trypsinized, treated with 0.075 M KCl for 15 min at 37°C, and fixed with methanol-acetic acid (3:1). Cell suspensions in fixative were dropped onto slides and air-dried. The slides prepared were stained with 5% Giemsa solution (Merck, Germany) and examined with a light microscope using a 100× objective lens. Sexing of individual aES cell lines was performed by PCR using an X chromosome-specific gene *Xist* (Zuccotti and Monk, 1995) and a Y chromosome-specific gene *Zfy* (Kay *et al.*, 1994) as reported (Obata *et al.*, 2000). DNA from the fetuses was processed using Qiagen kits as earlier. The primer sequences and PCR conditions for the amplification of all target genes are shown in Supporting Information Table 1. For EB formation, aES cells were digested with 0.05% trypsin, resuspended in the ES cell culture medium (Shinmen *et al.*, 2007) containing 15% fetal bovine serum without leukemia inhibitory factor and were cultured under feeder-cell-free conditions.

All procedures were reviewed and approved by the Animal Experimental Committee at the RIKEN Institute and were performed in accordance with the institute's guideline.

ACKNOWLEDGMENTS

The JF1 strain (*M. m. molossinus*) used in this study was provided by RIKEN Bioresource Center, with the support of the National BioResources Project of MEXT, Japan.

LITERATURE CITED

Barlow DP, Stoger R, Herrmann BG, Saito K, Schweifer N. 1991. The mouse insulin-like growth factor type-2 receptor is imprinted and closely linked to the Tme locus. Nature 349:84–87.